ADVANCED FUNCTIONAL MATERIALS
www.afm-journal.de

Light-Guiding Biomaterials for Biomedical Applications

*Soroush Shabahang, Seonghoon Kim, and Seok-Hyun Yun**

Optical techniques used in medical diagnosis, surgery, and therapy require efficient and flexible delivery of light from light sources to target tissues. While this need is currently fulfilled by glass and plastic optical fibers, recent emergence of biointegrated approaches, such as optogenetics and implanted devices, calls for novel waveguides with certain biophysical and biocompatible properties and desirable shapes beyond what the conventional optical fibers can offer. To this end, exploratory efforts have begun to harness various transparent biomaterials to develop waveguides that can serve existing applications better and enable new applications in future photomedicine. Here, the recent progress in this new area of research for developing biomaterial-based optical waveguides is reviewed. It begins with a survey of biological light-guiding structures found in plants and animals, a source of inspiration for biomaterial photonics engineering. The review then describes natural and synthetic polymers and hydrogels that offer appropriate optical properties, biocompatibility, biodegradability, and mechanical flexibility have been exploited for light-guiding applications. Finally, perspectives on biomedical applications that may benefit from the unique properties and functionalities of light-guiding biomaterials are discussed briefly.

1. Introduction

Optical waveguides are indispensable in many of today's technologies for telecommunication, manufacturing, aerospace, medicine, defense, and science. Waveguides enable us to confine light within narrow conduits and deliver it with minimal loss over long distances and around corners. Beyond optical transmission, waveguides can also serve as a platform for functional devices in which the intensity, polarization, or spectrum of light is altered in a desired manner by interacting with the waveguide materials and external environments.

Among optical materials, silica glass (SiO_2) has excellent transparency in the visible and near-infrared spectral range, high mechanical strength, and chemical inertness. These properties make silica optical fibers a leading choice for both long-haul optical telecommunication and short-distance data interconnection. Silica fibers are also widely utilized in medical settings, delivering laser light for surgery and catheter-based endoscopy. While the medical applications of silica optical fibers have been established, demands for new types of waveguides continued in medicine as the utilities of light in healthcare, diagnosis, therapy, and surgery increased and became more sophisticated.[1] For instance, for mid-infrared laser ablation of tissues, new fiber materials[2] and guiding structures[3] with lower optical loss than the silica fibers in the mid-infrared range are needed. It has been envisioned that many applications of photomedicine may benefit from nonconventional optical fibers that are more elastic, more biocompatible, and even biodegradable. Several biomaterials have been proposed to meet these requirements.

In this article, we review various biomaterials that can offer adequate optical properties to guide light and, simultaneously, provide desirable biophysical, chemical, and biocompatible properties not offered by conventional solid-state materials such as the silica glass and hard plastics. We begin this review by presenting some notable examples of biological optical waveguides found in living organisms. We then describe various recent examples of bio-inspired waveguides, material-inspired optical fibers, and need-driven waveguide-based devices. Finally, we discuss the potential of light-guiding biomaterials for biomedical sensing, diagnostic, and therapeutic applications.

1.1. Natural Optical Waveguides in Living Organisms

Life on Earth depends on sunlight from energy harvesting to optical vision. Through biological evolution, light-collecting and guiding structures emerged in various organisms. Many plants and animals employ specific types of optical waveguides to facilitate photosynthesis and visual acuity. These structures give benefit to the organisms for their fitness and survival.[1] The recent advances in our understanding about the role of biological waveguides have been a source of inspiration for the development of bio-mimicking waveguides.[4]

Photosynthesis in plants and small organisms such as algae converts sunlight energy to chemical energy. The stored chemical energy can later be released to fuel the organisms' activities and fed into animals providing them with vital energy. In certain environments, some plants have evolved specific optical structures to harness sunlight. For instance, Begonias grow on the floor of Asiatic forests where direct sunlight is scarce.

Dr. S. Shabahang, Dr. S. Kim, Prof. S.-H. Yun
Wellman Center for Photomedicine
Massachusetts General Hospital
Department of Dermatology
Harvard Medical School
65 Landsdowne Street, Cambridge, MA 02139, USA
E-mail: syun@hms.harvard.edu
The ORCID identification number(s) for the author(s) of this article can be found under https://doi.org/10.1002/adfm.201706635.

DOI: 10.1002/adfm.201706635

The shade-dwelling Begonias have photonic-crystal-shape iridoplasts that increase the chance of absorbing the photons, a working strategy for survival under the low-light condition.[5] Other type of Begonia employs an additional scheme: their epidermal cells at the surface of leaves are transparent and have a convex shape that focuses feeble sunlight onto the grains of mesophyll,[6] which improves light harvest at the sunlight-scarce ground of the forest.[7] Sclereids in the evergreen sclerophyll *Phillyrea latifolia* form a vertically oriented foliar structure that delivers photons to mesophyll (**Figure 1**a). About 40–80% of photons arriving at the spongy mesophyll region is collected by the presence of the waveguiding structure, an about 30-fold increase compared to mesophyll cells located far from the waveguides.[8]

In Lithops and Haworthia plants, known as "living stones," transparent windows on the upper part of the plant allow sunlight to penetrate deeper into leaves (Figure 1b). Along the leaves, chlorophyll is increasingly concentrated toward the bottom (Figure 1c). This positive gradient of absorbers counteracts with the negative gradient of optical intensity so that light absorption occurs uniformly throughout the entire region of the leaves. This arrangement ensures high photosynthesis yield while avoiding localized absorption at the top of the leaves, which can cause photothermal damage during hot, dry days.[9]

Besides photosynthesis, plants use sunlight for other processes critical for survival and growth. Light can coordinate various processes ranging from seed germination to plant blooming, root growth angle with respect to gravity and sunlight direction, and even elongation and expansion speed of stems and leaves.[10] Plants have several types of sensory photoreceptors. Some photoreceptors are present in roots under the ground and enable the roots to sense light from the UV-B to far-red spectrum.[11] The root receives light stimuli through both diffusion in the soil and transmission along their vascular system that serves as natural optical waveguides. The vascular system in plants transports water and minerals from roots to leaves and distribute photosynthesized glucose from leaves to other parts of the plant. The water pipes of the vasculature capture some light that enters the stem and propagate it to the photoreceptors in the roots under the ground[12] (Figure 1d–g). Spectral measurements revealed that far-red light was transported most efficiently through the vascular pipes.[11] Another study showed that the underground roots of *Arabidopsis thaliana* can receive stem-guided light and sense the aboveground light environment during plant environmental adaptation.[13] In the roots, the transported light can photoactivated phytochrome B, which triggers the expression and accumulation of elongated hypocotyl 5 protein, resulting in the light-induced root growth response.

Bioluminescence has been widely observed in marine vertebrates, invertebrates, fungi, and microorganism species. These animals, especially living in deep ocean, benefit from bioluminescence for luring their prey, attracting mates, scaring off predators, communicating, camouflaging, and even illuminating nearby area to visualize.[14] The photons generated from bioluminescence organs are often guided by some waveguiding structures and emitted out in specific patterns. For instance, jellyfish are mostly made of a translucent gel-like substance called mesoglea, with large water content of 95–98%.[15] Some bioluminescence light is guided through optical-fiber-like tentacles (Figure 1h), which jellyfish use as a decoy to attract prey.[16]

In insects, vision is achieved in compound eyes that are composed of hundreds and thousands of tiny corneal lenses on the surface of the eye. Each corneal lens focuses light into an individual light-detecting structure consisting of several photoreceptor cells (retinula cells), through crystalline cones called ommatidia. Each ommatidium is typically 5–50 μm long and

Soroush Shabahang obtained his Ph.D. in optics and photonics from CREOL, the College of Optics & Photonics at the University of Central Florida in 2014. He is currently a research fellow at the Wellman Center for Photomedicine, Harvard Medical School. His research interests include multi-material specialty optical fibers and his current research is focused on optical waveguides and devices for biomedical applications.

Seonghoon Kim received his Ph.D. degree from the Korea Advanced Institute of Science and Technology (KAIST) in 2015. He is currently a postdoctoral fellow at Harvard Medical School and Massachusetts General Hospital. His research interests include the biomaterial based optics and photomedicine.

Seok-Hyun (Andy) Yun received his PhD in Physics in 1997. His thesis research on fiber-optic devices led to a venture-funded telecom startup in Silicon Valley, where he managed engineering prior to acquisition. He joined Wellman Center for Photomedicine at Massachusetts General Hospital in 2003 as Instructor. Currently, he is Patricia and Scott Eston MGH Research Scholar and full Professor at Harvard Medical School, an affiliated member of faculty of MIT, and the Director of Harvard-MIT Summer Institute for Biomedical Optics. His research areas include optical imaging, photomedicine, biomaterials photonics, and biological lasers.

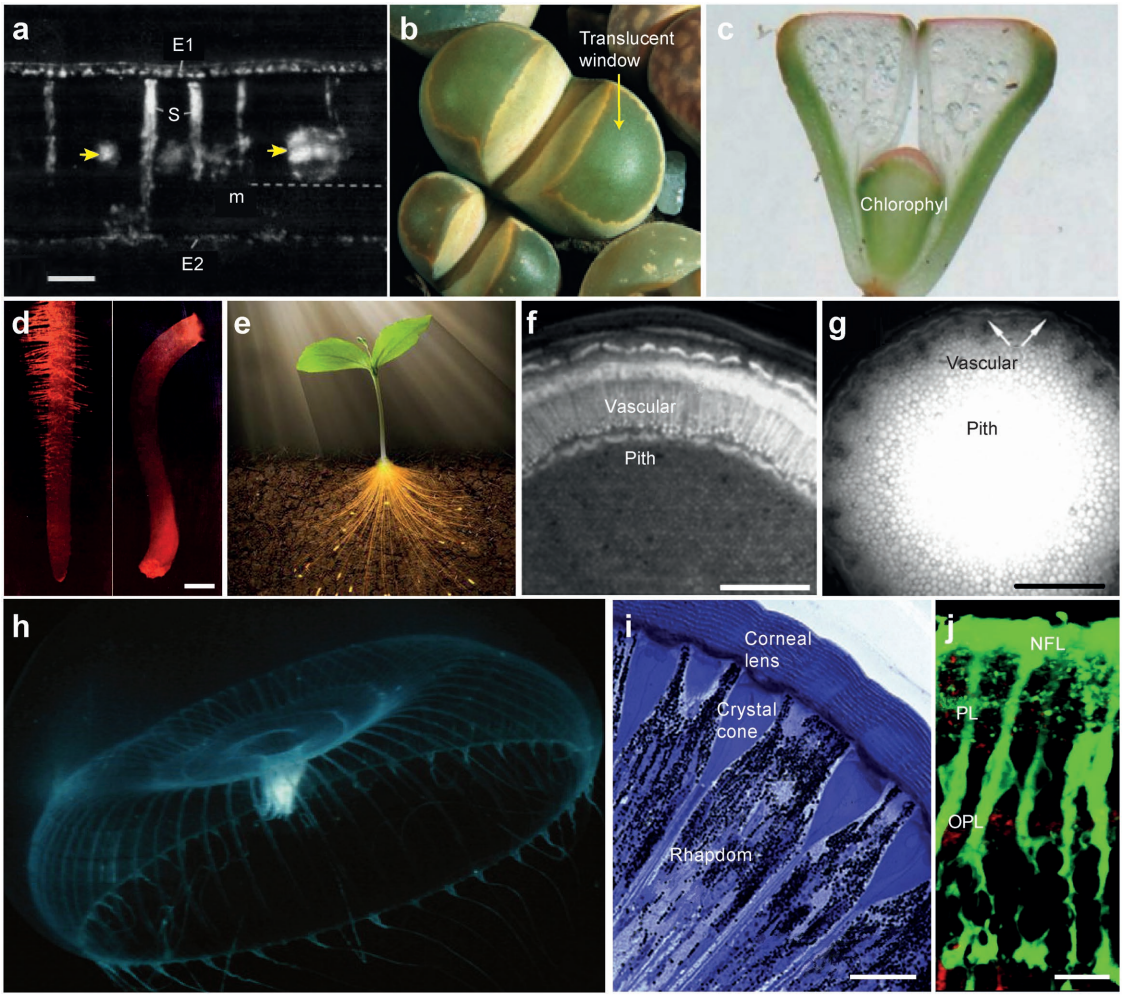

Figure 1. Optical waveguiding structures in living organisms. a) Hand-cut transverse section of a mature leaf of *P. latifolia* under polarized light. E1: adaxial epidermis, E2: abaxial epidermis, m: mesophyll, S: osteosclereids. Yellow arrows indicate veins, and the dotted line indicates the paradermal section. Scale bar, 100 µm. Reproduced with poermission.[8] Copyright 2011, Society for Experimental Biology. b) *Lithops olivacea* with green bodies and large pinkish translucent windows through which sunlight penetrate into the leaf.[9] c) Fenestrated *Haworthia* and *Lithops* with translucent tissues.[89] d) Optical images of red laser light guided in (left) in a corn root and (right) in an oat seedling.[10] Scale bar, 1 mm. e) Artistic drawing of a plant, illustrating light guiding through the stem to the roots.[13] f) A cross-section image of the stem of a 1-year-old *Aesculus turbinate*. More efficient light guiding in the vascular tissue than in pith.[12a] Scale bar, 1 mm. g) A cross-section image of the stem of a *Fallopia japonica var. uzenensis*. More efficient light conduction in pith than in vascular bundles.[12b] Scale bar, 1 cm. h) An inch-long jellyfish emitting bioluminescence light guided through its transparent tissues.[90] i) A cross-section imaging showing the longitudinal organization of ommatidia in *Australian desert ant*.[91] Scale bar, 10 µm. j) A cross-sectional fluorescence imaging of a pig retina tissue slice, showing Muller cells stained with a fluorescent dye (green). IPL: inner plexiform layer, OPL: outer plexiform layer, NFL: nerve fiber layer.[20a] Scale bar, 10 µm. Figures reproduced with permission from: (a) ref. [8], Copyright 2011, Society for Experimental Biology; (b) Copyright 2010, Quae edtions. (c) ref. [89] Copyright 2014, Museo Civico di Rovereto; (d) ref. [10], Nature Copyright 1984, Scientific American Inc.; (e) ref. [13], The Copyright 2016, American Association for the Advancement of Science; (f) ref. [12a] Copyright 2003, Society for Experimental Biology; (g) ref. [12b], Copyright 2004, Society for Experimental Biology; (h) ref. [90], Copyright 2010, Annual Reviews; (i) ref. [91], Copyright 2001, Elsevier; (j) ref. [20a], Copyright 2007, National Academy of Science.

a few microns wide and serves as an optical waveguide connecting the lens to the light-sensitive sensory region of retinula cells (rhabdom) (Figure 1i).[17] The ommatidium is categorized into two types: photopic, which characterizes insects active during the daytime, and scotopic, which characterizes nocturnal insects. In the photopic type, the base of the crystalline cone is in contact with the rhabdom, but in the scotopic type there is space, called the clear zone, between the crystalline cone and the retinula cells. Under abundant light, scotopic ommatidium acts the same as photopic ommatidium, but in a dark environment the shielding pigments between scotopic ommatidia contract and allow the light to leak into the rhabdom of adjacent ommatidia, leading to visual sensitivity enhancement.[18]

In vertebrate' eyes, the transparent cornea and lens form an optical image onto the retina. Once optical rays enter the retina tissue, they must pass through several layers of cells before reaching photoreceptor cells. The optical refraction and scattering in the retinal tissue tend to distort the optical image. It has been found that Müller glial cells, in addition to their primary role in facilitating cell–cell connection between nerve cells in the

retina,[19] serve as optical fibers helping image projection through the retinal tissue with less image distortion and light scattering loss (Figure 1j).[20] In the human eye, Müller cells have a length of up to ≈150 µm and a width of ≈12 µm at the top and 2–3 µm in the middle. Müller glial cells have a refractive index (RI) of ≈1.38, slightly higher than their surrounding cells, allowing light to be guided through their tube-like cell body extending from the retinal surface to the midsection of photoreceptor cells. Remarkably, the spectral properties of Müller cells are optimized for photopic and scotopic vision. The green-red part of the visible spectrum is delivered to cones that are responsible for color vision, and the blue-purple part of spectrum is leaked nearby rods. This arrangement maximizes photon absorption by cones while minimally affecting rod-mediated vision.[21]

1.2. History of Optical Waveguides

One of the first scientific description of optical waveguiding dates back to 1841, when Colladon and his students demonstrated guiding of sunlight through a flowing water jet.[22] In 1842, Babinet demonstrated guiding of candlelight through a glass bottle and a curved glass rod.[23] Tyndall studied internal reflection angles in water jets[24] and is credited for the discovery of total internal reflection. With the electromagnetic theory of Faraday and Maxwell in the late 19th century, the scientific basis of optical waveguides has been established. Soon after, various waveguides were devised for other applications.[25] William Wheeler in 1891 devised a lens-based light pipe system to transport arc lamp light for home lighting.[26] The first use of an optical waveguide for medical applications was by Roth and Reuss in 1889. They utilized glass rods to illuminate tissues in the larynx and nose during surgery.[27]

DuPont developed commercial polymethyl methacrylate (PMMA), marketed as Lucite and Pexiglas, in 1937 (**Figure 2**a).[28] This thermoplastic polymer was commonly used during World War II for airplane windshields, canopies, bomber noses, submarine periscopes, and gunner turrets due to its high transparency, low density, and durability against wind, water, and UV rays. In 1939 Curvlite Sales developed a PMMA optical waveguide for dental illumination (Figure 2b).[29] This might be the first use of a polymer optical waveguide for medical applications. Thereafter, many different transparent polymers have been developed.

The first single-mode waveguide that supports only one spatial mode was demonstrated in 1959[30] by drawing silica glass into a narrow fiber with its core size in the order of the optical wavelength (λ). For waveguides consisting of a core diameter d and refractive index (RI) n_{core} and a cladding RI n_{clad}, the number of guided modes is approximately equal to $\sim 5(d/\lambda)^2(n_{\text{core}}^2 - n_{\text{clad}}^2)$. Single-mode waveguides are preferred over multimode waveguides for sending optical signals over a long distance for telecommunication. In multimode waveguides, different spatial modes travel at slightly different speeds. As a result, signal is distorted over propagation length. In 1961, Goubau proposed hollow optical waveguides with regularly spaced phase-correcting plates, lenses or mirrors, but this idea did not receive much attention due to high loss and complexity in fabrication.[31]

With the development of semiconductor lasers in early 1962 and the vision for long-distance optical telecommunication

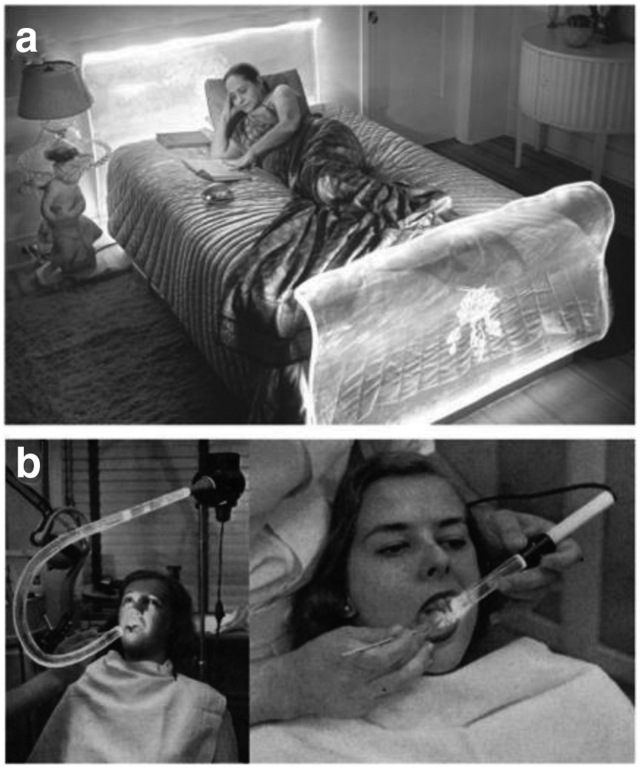

Figure 2. Early forms of light pipes: a) Lucite headboard designed by Ladislas Medgyes in the late 1930s, with fluorescent light for nighttime reading. Reproduced with permission.[28] Copyright 1995, Rutgers University Press. b) Lucite optical waveguides in 1930s providing sterile beams devoid of heat, glare, or the danger of electrical shock, carries light around curves and bends. Reproduced with permission.[29] Copyright 1939, Bonnier Corporation.

motivated scientists to look for low-loss optical materials and develop optical waveguides that could be produced in a long length at low cost. Until 1970s, the material loss of silica fibers was over 1000 dB km^{-1}, limiting the maximum transmission length to a few meters. Based on a careful spectroscopic analysis of silica glass, Jones and Kao in 1966 reported that the optical loss of silica glass can be made smaller than 20 dB km^{-1} by removing impurities and proposed silica-based core-clad single-mode optical fibers for telecommunications.[32] For this pioneering work, Kao was awarded the Nobel Prize in Physics 2009. With the technical advances in glass purification, preform deposition, and fiber drawing, the state-of-the-art silica fibers have a loss of 0.2 dB km^{-1} at the third optical telecom window around 1550 nm.

Nowadays, numerous specialty optical fibers and waveguides with specific optical properties and different guiding structures[33] have become available for scientific, industrial, and military applications. Besides silica and plastics, researchers are investigating various other solid-state materials including chalcogenide glasses, semiconductors, ceramics, and metals.[34]

While the medical applications of the solid-state optical waveguides have been established, the recent expansion of biotechnologies and bioengineering and the recognition of the potential benefits of waveguides with tissue-like properties, such as biocompatibility, biodegradation, and elasticity,

have motivated scientists and engineers to pay their attention to optically transparent biomaterials. Further, biological optical waveguides found in living organisms inspired researchers to learn from the Nature's indigenous waveguide designs for in vivo use. As a result, many different types of man-made optical waveguides have been developed in the past several years. In the sections below, we describe the recent advances in the development of novel optical waveguides made with natural and synthetic biomaterials with desired characteristics.

2. Properties of Optical Biomaterials

According to the U.S. National Institutes of Health, biomaterials are defined as "any substances that are obtained from nature or synthesized in the laboratory for biomedical purposes or in contact with biological systems." Biomaterials include ceramics, metals, glasses, polymers, biological tissues, cells, and any other materials that are nontoxic, noncarcinogenic, nonthrombogenic, and nonimmunogenic.[35] Biomaterials are used in various implantable biomedical devices, such as hips joints, intraocular lenses, artificial hearts, breast implants, and hearing valves.[36]

While conventional optical materials, such as glass, plastics, and crystals are well known, many of these materials are not biocompatible and can cause chemical toxicity. Furthermore, waveguides made of these solid-state materials are much stiffer than biological soft tissues and must be removed from the body after use because they can mechanically damage tissues. To overcome these problems, researchers turned to biomaterials that are softer yet tough, like tissues, and either bioinert or biodegradable, while having sufficient transparency to transmit light over a desired length.

Soft biomaterials have polymeric structures, consisting of numerous polymers of varying lengths interconnected by covalent or ionic crosslinks, pi–pi stacking, and physical entanglement. Each polymer chain in the polymer network can rotate and bend relatively freely with respect to their neighboring units. This kinetic degree of freedom imparts softness to the polymeric material. Shear and Young's moduli describe the resistance of material to deformation. In the simple Kuhn's model of rubber, the mechanical moduli are proportional to the number of crosslinks per volume or crosslinking density.

In polymeric biomaterials, the optical loss arises from a few distinct origins. The first loss mechanism is absorption of photons by constituent molecules. Organic molecules can strongly absorb short wavelengths below 350–400 nm. Certain organic molecules have a linear or circular chain of carbon atoms with delocalized electrons through combined p-orbitals. This conjugation system can have an absorption peak in the visible spectrum. In general, conjugated polymers are not considered as a candidate for optical waveguides since optical absorption is undesirable for light delivery. However, as we will see below, small conjugated molecules, such as dyes and fluorophores, may be incorporated into optical waveguides for specific functionalities, such as biomolecular sensing, optical amplification, and strain measurement.

The second loss mechanism is light scattering. In a single crystal with perfect periodic arrangement of atoms, light can propagate without any loss in principle. In crystals with defects or glasses with amorphous structures, light scattering arises from the structural imperfections. Since the size of the inhomogeneity is at the atomic scale, much smaller than the optical wavelength, this type of scattering is called Rayleigh scattering and have a magnitude proportional to $1/\lambda^4$, decreasing rapidly with increasing wavelength. This wavelength dependence is a part of the reason why current long-haul fiber-optic communication uses long-wavelength near-infrared light near 1550 nm. In state-of-the-art silica fibers with low impurities, the optical transmission loss limit is imposed by Rayleigh scattering in the amorphous glass.

In polymeric biomaterials, however, additional structural inhomogeneity arises from the partially disordered network of long polymer chains and macromolecules. The sizes of the inhomogeneity are no longer limited to the atomic scale but extend to tens of nanometers to micron scales. When the size scale is greater than about one tenth of the optical wavelength, relatively strong Mie-type light scattering occurs. The magnitude of Mie scattering in polymeric materials can be several orders of magnitude stronger than Rayleigh scattering in transparent solid-state glasses and crystals. Nevertheless, unlike long-haul optical telecommunications, the distance of interest in most biomedical applications is generally in the range of 1 mm to 1 m at most. Some biological tissues are naturally transparent. The cornea and crystalline lenses in the eye are representative examples. The optical loss in these tissues is an order of 1 dB cm^{-1}. Although this level of transparency is sufficient to ensure good transmission to the retina, it is in fact 5 orders of magnitude lower than the silica glass. Commonly encountered transparent soft biomaterials have a loss coefficient in the range of 0.3–1 dB cm^{-1}. It will be a worthwhile challenge for material scientists to develop biomaterials with a low loss of <0.1 dB cm^{-1}, yet providing desired mechanical and biochemical properties. In the next section, we discuss a number of soft polymeric biomaterials that offer acceptable transparency for light delivery over a length of 1–10 cm and mechanical modulus similar to native tissue simultaneously. From the standpoint of transmission distance, light scattering is undesirable, but it may be a useful design factor. For example, suppose an application that requires a spatially extensive delivery of light along an implanted waveguide. In this case, designed and controlled scattering through the waveguide can be an effective mechanism to extract light from the device to the surrounding tissues.

The third type of loss is waveguide loss. A waveguide loss can arise from several different causes including surface roughness, which cause light scattering, and micro and macroscopic bending of the waveguide. Light leakage through optical refraction from the waveguide to surrounding medium is another source of waveguide loss. In an ideal situation, total internal reflection is the primary mechanism of optical waveguiding. However, the condition for total internal reflection condition can be partially disrupted by microscopic or macroscopic perturbations along nonideal waveguides.

Besides optical transparency, the RI of optical materials plays an important role in determining the waveguide loss and, therefore, the efficiency of light guiding. For single-material waveguides, the RI of the material must be higher than that of the surrounding tissue for total internal reflection to occur. The RI of a material originates from molecular dielectric polarizability or the displacement of bound electrons by the electromagnetic field of light. Although the polarizability and RI of a material vary in principle at the atomic and molecular level, it is practically

Table 1. Various polymeric biomaterials that have been used for biocompatible waveguides and their material properties reported in literature.

Material	Refractive index	Optical loss [dB cm^{-1}]	Young's modulus	Maximum elongation [%]	Biodegradation speed	References
Silkworm silk	1.54–1.55	0.1–28	3.8–17 GPa	4–33.3	10 min to 1 month	[4b,40b,41,88,94]
Spider silk	1.5–1.7	0.7–11	1–24 GPa	4–30	2–3 weeks	[43,93,95]
Agarose gels, alginate gels, gelatins	1.34–1.54	0.3–13	30–80 kPa	700–2000	1 h to 8 weeks	[4e,h,50-51,58,96]
Cellulose	1.475	0.1	–	20–70	A few months	[68,97]
Chitosan	1.38–1.54	0.8–7.3	1.3 GPa	3	2–12 months	[71,98]
PLA, PLLA, PDLA	1.46–1.47	1.5	2.7–7 GPa	3–100, nonelastic	1 week to 4 months	[4b,69,99]
PGA	1.45–1.51		6.5 GPa	25, nonelastic	1 week to 5 months	[99e,100]
PLGA (50/50)	1.47–1.61		0.7–7 GPa	7–20, nonelastic	1 week to 6 months	[4b,99c,101]
POMC and POC	1.49–1.54	0.4	4.7–6.1 MPa	57–103	~1 month	[67]
PEG hydrogels	1.35–1.47	0.17–25	1–44 kPa	300–2000	Nontoxic, inert, nonabsorbable	[4g,102]
PAM hydrogels	1.46–1.50	1–11	20–27 MPa	13–74		[4d]
PDMS	1.41–1.47	0.5	0.57–3.7 MPa	95–140		[4c,74a,78,86,103]
Polyurethane	1.46	2	0.3 MPa	10		[81]
COCE	1.51	4	34 MPa	230		[86]

defined as a spatially averaged quantity over the dimension of the optical wavelength. The RI (n) of a tissue can be expressed as[37]

$$n = n_{\text{dry}}(1-W) + n_{\text{water}}W$$

where n_{dry} (≈1.51) is the RI of tissue's dry mass, n_{water} (≈1.33) the RI of water, and W is the water content of the tissue. For biological tissues with a typical water content $W \approx 0.7$, the RI would be ≈1.38. Actual measured RI of various tissues at visible wavelengths are in the 1.38–1.41 range. The above equation is also valid for synthetic biomaterials, particularly hydrogels, for which n_{dry} depends on the specific material composition. However, most organic materials have similar n_{dry}.

Besides the mechanical and optical properties, the chemical and biological properties of biomaterials are crucial for biomedical waveguides. Several natural materials are suitable for this purpose. However, a wide range of synthetic polymers and hydrogels can be tailored to meet the needs. Some representative biomaterials are summarized in **Table 1**.

3. Biomaterial-Based Optical Waveguides

3.1. Biological Materials

The discovery of light-guiding Müller cells inspired researchers to build optical waveguides from biological cells. This is largely curiosity-driven research, but cellular waveguides may have some practical relevance to biophysical studies of cells and potentially tissue engineering. Bezryadina et al.[38] investigated light propagation through cyanobacteria, and demonstrated intensity-dependent light guiding efficiency (**Figure 3**a). Xin et al.[39] reported the formation of optical waveguides via optical trapping of live *Escherichia coli* bacteria cells in aqueous solution along the beam path (Figure 3b). The RI of *E. coli* cells are ≈1.39, higher than the water (≈1.33), thus allowing light to be guided through the chain of cells over several tens of μm by total internal reflection at the interface of the cell membrane and the water. Humar and Yun[4f,i] inserted spherical optical resonators, such as droplets of bioinert oil, lipid droplets, and polystyrene microbeads, into cells and demonstrated the generation of whispering gallery modes (WGM) and intracellular lasing. (Figure 3c)

Silk fibers, a natural polymer produced in silkworms and spiders, have been exploited as a biocompatible optical material. Silk offers excellent biocompatibility and tunable biodegradability, and can form substrates with optically uniform and smooth surfaces. In addition, good mechanical strength and optical clarity makes silk an excellent optical biomaterial.[40] Omenetto and Kaplan[40a] fabricated lenses, micro-lens arrays, diffraction gratings, and pattern generators out of silk proteins obtained from silkworm cocoons by boiling in LiBr solution and then dialyzing in aqueous solution (**Figure 4**a). Lawrence et al.[41] controlled surface morphology down to 125 nm to fabricate 2D diffraction gratings, and Perry et al.[42] constructed 3D silk fibroin-based nano- and micropatterned films. Optical waveguides have been fabricated from silk. Parker et al.[40b] developed a technique to print out silk optical waveguides on glass from silk fibroin solutions. The waveguides showed 0.1 dB cm^{-1} propagation loss in the air/glass interface due to the relatively high RI (≈1.54) of the silk and can guide visible wavelength light over centimeters (Figure 4b). Besides the silkworm silk, spider silk proteins have also been used for optical waveguides (Figure 4c). Qiao et al.[43] fabricated optical fibers with recombinant spider silk proteins (Figure 4d). Core-only fibers without a cladding tend to suffer from waveguide loss in tissue by scattering due to microscopically inhomogeneous RI of the surrounding tissue.[37] To resolve this issue, a step-indexed core-cladding silk optical waveguide was proposed in which the core was a silk film and the cladding was a silk hydrogel (Figure 4e).[44] The propagation loss of the core-clad fibers were smaller than the core-only fibers and less sensitive to the surrounding environment.

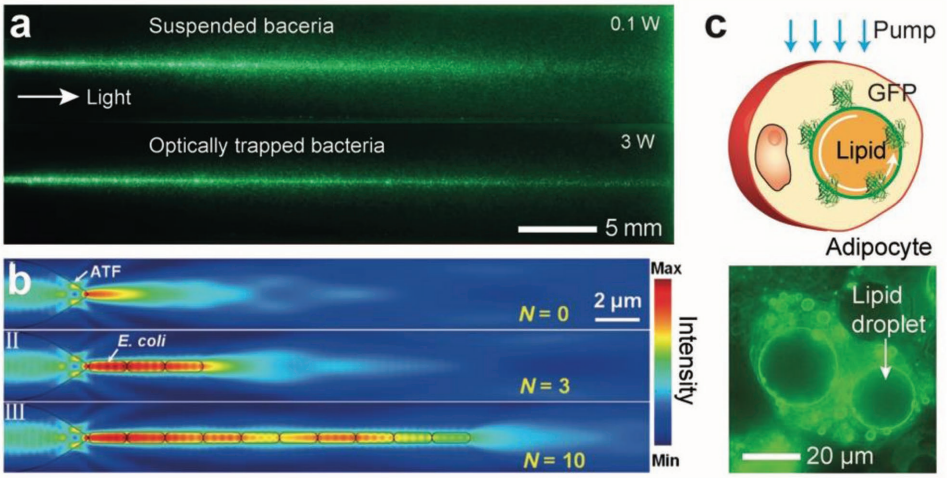

Figure 3. Optical waveguides made from biological cells. a) Pictures showing light scattering of a laser beam propagating in seawater containing suspended *Synechococcus cyanobacteria* when the optical power is low (top) or high (bottom) enough to optically trap the tiny bacteria along the beam so that they form a light guide.[38] b) Simulation of optical trapping of *E. coli* bacteria by a laser beam light and light propagation.[39] c) Adipocyte cells containing lipid droplets that generate WGM optical resonance.[4i] Figure reproduced with permission from: (a) ref. [38], Copyright 2017, American Physical Society; (b) ref. [39], Copyright 2013, American Chemical Society; (c) ref. [4i], Copyright 2017, Optical Society.

3.2. Hydrogels

Various types of hydrogels have been explored for flexible, biocompatible optical waveguides. Hydrogel is a crosslinked network of hydrophilic polymers and contains water in its nano- and micron-size pores. The optical and mechanical properties of hydrogels can be controlled by adjusting their polymer content, molecular weights, and crosslinking density and can closely match those of soft tissues, which will help to avoid a mechanical damage on tissue and also improve cell viability properties. Mazzoccoli et al.[45] reported mechanical and cell viability properties of various molecular weight PEG diacrylate (PEGDA) blended hydrogels (**Figure 5**a,b). The magnitude of shear modulus of a hydrogel increases with increasing crosslinking density and can cover the typical range of tissues from 1 kPa to 1 MPa. Hydrogels made with biocompatible polymers are an excellent scaffold for tissue engineering.[46] The degree of crystallinity and the size of crystallite of hydrogels are a function of water content and molecular weight of polymers. Therefore, hydrogels can be optically transparent with a material loss of 0.1–1 dB cm^{-1} by choosing appropriate polymer chain lengths and water content. For example, hydrogels are typically transparent and flexible when the water content exceeds 70% and their precursor molecular sizes are greater than ≈1 kDa (Figure 5c–e).[4g] As described earlier, the RI of a hydrogel is variable with the water content (W) in a range from ≈1.34 ($W \approx 1$) and 1.54 ($W << 1$).

In addition, the presence of water-swollen pores in hydrogels makes it relatively easy to incorporate functional molecules into the network. The pore size can be controlled by varying the molecular size of polymer precursors and the water content. Depending on the pore sizes, desired biomolecules such as specific proteins, nutrients, and chemical substances can be embedded physically or covalently into hydrogels. With the tissue, the trapped molecules can be released and diffused out of the hydrogels. This feature makes hydrogels an attractive choice of material to make functional biophotonic waveguides providing drug delivery and controlled drug release.[47] Furthermore, hydrogel swelling capacity is subject to change by environmental variation of pH, temperature, ion concentration, surfactants, ligand attachment, degree of crosslinking, and interaction with other molecules. The variable swelling property may be harnessed for hydrogel-based optical waveguide biosensors (Figure 5f).

Natural polymers, such as polysaccharides and protein fibers, can form hydrogels. Alginate gels, agarose gels, and collagen-derived gelatin have been widely investigated for tissue regeneration scaffolds[48] and long-term cell encapsulation.[49] A number of step-index optical waveguides made of natural hydrogels have been demonstrated. Manocchi et al.[50] demonstrated a 2D optical waveguide with a biocompatible and biodegradable gelatin core (n = 1.54) and agarose cladding (n = 1.50) using layer-by-layer spin-coating on a plastic substrate. The cladding layer improved light transmission efficiency. Jain et al.[51] demonstrated an agarose hydrogel-based optofluidic platform for incorporation of biomolecules and cells (**Figure 6**a).

Polyethylene glycol (PEG) has been one of the most promising biomaterials in drug delivery, tissue engineering, and surface coating of nanoparticles due to its outstanding biological properties. PEG has excellent biocompatibility, nonimmunogenity, resistance to protein adsorption, and high water-storage capacity. PEG hydrogels are commonly fabricated by crosslinking PEGDA in aqueous solution. Relatively higher RI and high optical transparency obtained over a broad range of precursor lengths and water content allows fabrication of PEG based hydrogel optical waveguides (Figure 6b).[4g] Within this range, the mechanical properties are tunable by adjusting the molecular weights and water content.[52]

Light-induced manipulation of cells has become more versatile and efficient by using optogenetic tools. Ye et al.[53] developed a synthetic optogenetic system to enhance blood-glucose homeostasis. However, its application to humans would be difficult because the optical intensity required to induce optogenetic effects on cells implanted under the skin

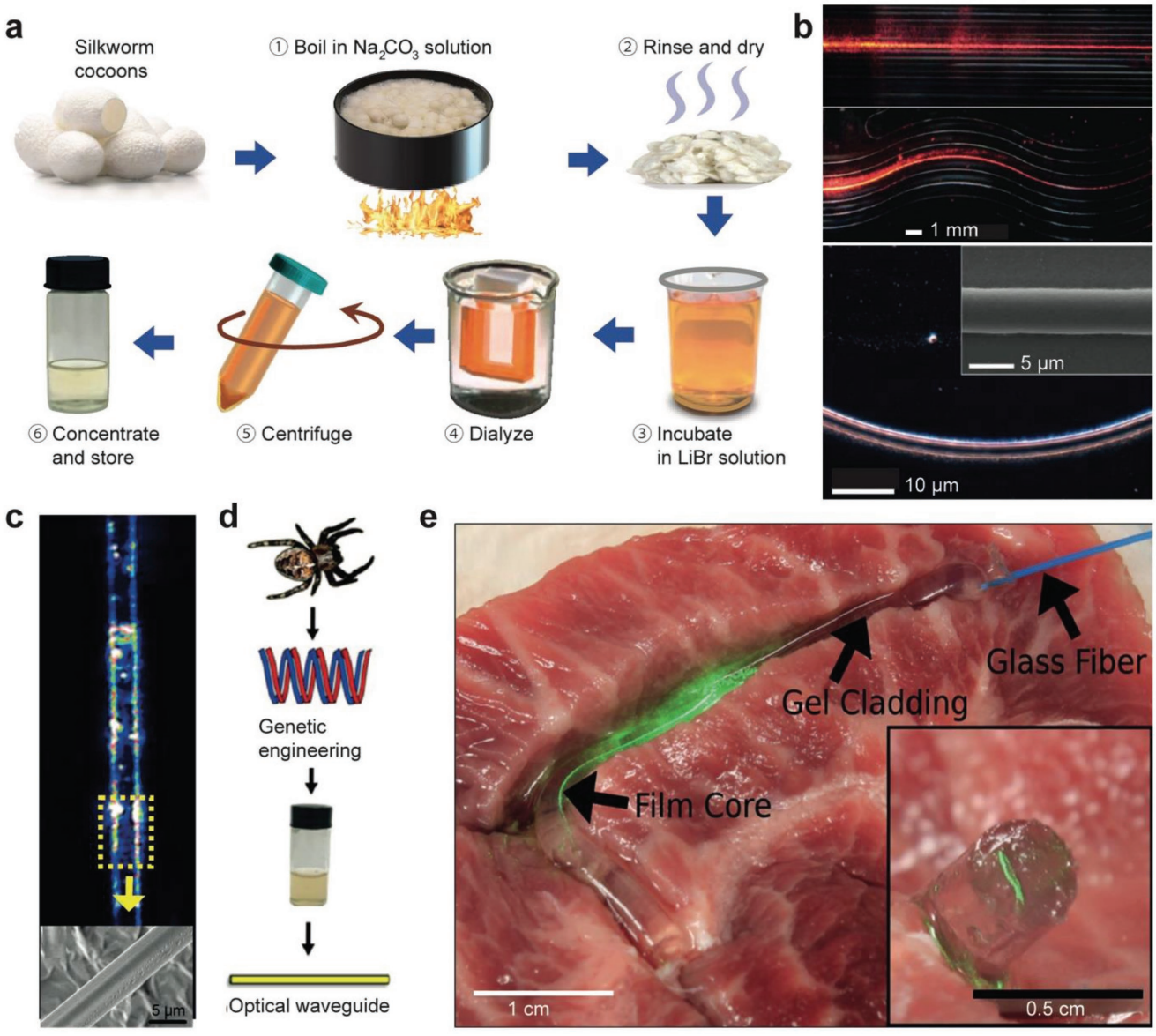

Figure 4. Optical waveguides made of silk. a) Silkworm fibroin preparation steps.[40a,43] b) Light propagation along silk waveguides directly written on a glass substrate.[40b] c) Light guiding along spider silk fibers.[93] d) Schematic of making an silk fibroin optical waveguide out of genetically engineered spider silk.[43] e) Demonstration of light guiding through a core/clad silk fiber in contact with a tissue.[44] Figure reproduced with permission from: (b) ref. [40b], Copyright 2009, Wiley; (c) ref. [93], Copyright 2013, American Physical Society; (d) ref. [43], Copyright 2017, American Chemical Society; (e) ref. [44], Copyright 2015, Optical Society of America.

exceeds the safety limit (0.2–4 W cm^{-2} in the visible to near-infrared range). To overcome this limitation, Choi et al.[4g] encapsulated optogenetically engineered cells within a PEG hydrogel waveguide (Figure 6c). For in vivo tests, they inserted the waveguide in the subcutaneous space in a mouse model. The hydrogel waveguide delivered blue light uniformly onto the encapsulated cells, and the optogenetic circuit of the cells was activated to produce and secrete glucagon-like peptide 1, a substance that helps the body respond to insulin. The hydrogel protected the cells from the host immune response and allowed the secreted therapeutic protein to diffuse to the surrounding tissue. As a result, the implanted hydrogel waveguide effectively regulated the blood glucose level of the diabetic mouse. Choi et al. also developed a PEG hydrogel incorporating green fluorescent protein reporter cells for cytotoxic stress and demonstrated the feasibility of continuous monitoring of quantum dot toxicity in vivo in mice using the optical waveguide implant.[4g]

Choi et al.[4h] further developed a core-clad hydrogel fiber using a PEG core and an alginate cladding. The PEG hydrogel core was made by crosslinking of a PEGDA monomer solution in a tubular mold and extracted after incubation in dichloromethane, and a cladding layer was added onto the core by dipping it in a sodium alginate and calcium chloride solution (Figure 6d). The hydrogel

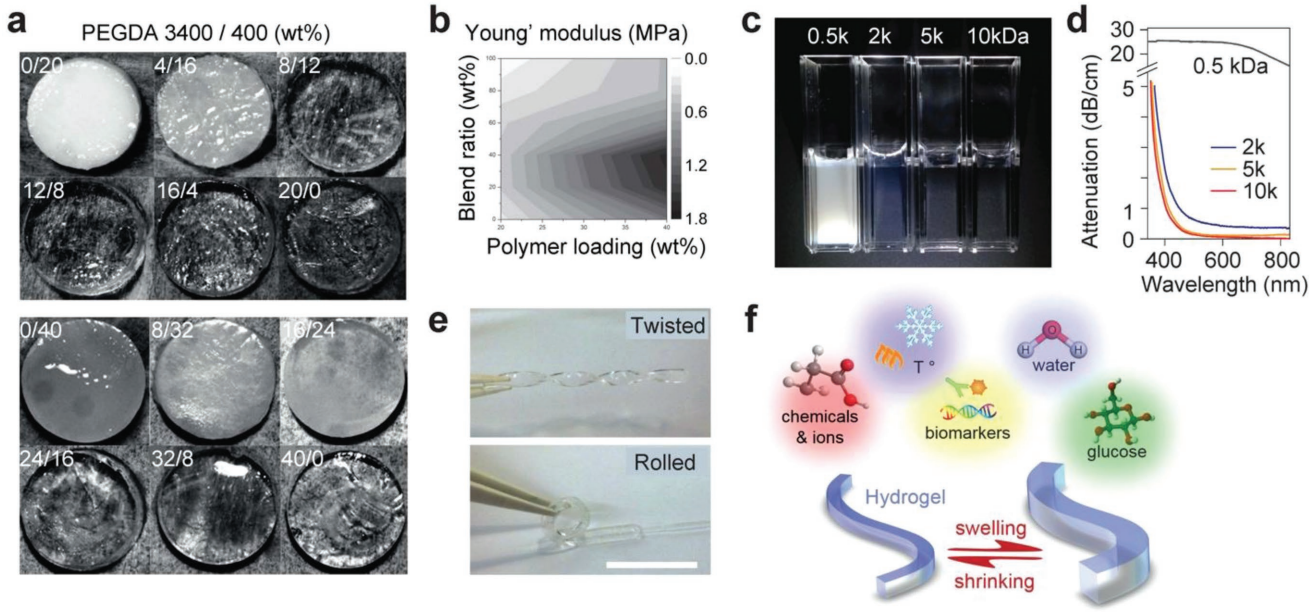

Figure 5. Optical and mechanical properties of hydrogels. a) Hydrogel discs with 20 wt% (top) and 40 wt% (bottom) polymer concentrations and various blending ratios of precursors with two different PEGDA molecular weights: 3400 and 400 Da. Different polymer concentrations and molecular weights result in different optical clarity.[45] b) A contour plot of measured Young's modulus of PEGDA hydrogels with respect to polymer concentration (horizontal axis) and blending ratio of PEGDA 3400/400 (vertical axis).[45] c) Comparison of PEGDA hydrogels made from 10 wt% PEGDA solution with molecular weights of 0.5, 2, 5, and 10 kDa, respectively.[4g] d) Optical attenuation spectra of the hydrogels depending on precursor molecular weights. e) Mechanical flexibility of a PEG hydrogel made of 5 kDa PEGDA at 10 wt%.[4g] f) Illustration of the stimuli-responsive swelling and shirinking property of hydrogels. Figure reproduced with permission from: (a) and (b) ref. [45], Copyright 2010, Wiley; (c–e) ref. [4g], Copyright 2013, Nature Publishing Group.

fibers are flexible and had a relatively low propagation loss of 0.3 dB cm^{-1} in the air and 0.49 dB cm^{-1} in a tissue (Figure 6e). The porous structure of hydrogels allows functional dopant molecules to easily enter the waveguide. PEG hydrogel fibers doped with Rhodamine 6G organic dyes produced amplified spontaneous emission and generated WGM lasing when the dyes were optically pumped at sufficient intensity levels (Figure 6f). The potential of hydrogel fibers for endoscopy and monitoring of oxygenated and deoxygenated hemoglobin concentrations in vivo have also been demonstrated in live mice (Figure 6g).[4h]

Polyacrylamide (PAM) hydrogel is a nontoxic, bioinert, and nonabsorbable biomaterial. Due to its flexibility, optical clarity, and long working lifetime, PAM is used in ophthalmic operations and plastic and aesthetic surgeries. PAM hydrogels have a potential for in situ monitoring of blood glucose levels.[54] Heo et al.[55] developed of an glucose-responsive hydrogel optical probe implantable in the skin and measured the concentration of interstitial glucose in a mouse model in vivo for a month. However, the optical readout through the intact skin layer was prone to errors[55,56] due to varying tissue properties.[57] To solve this problem, Yetisen et al.[4d] developed an implantable hydrogel optical fiber using a PAM-PEGDA block co-polymer hydrogel core and a calcium alginate hydrogel cladding. 3-Acrylamido phenylboronic acid molecules were covalently incorporated into the fiber core as glucose sensing receptors. As glucose molecules bind with the boronic acids, the swelling property of the hydrogel was altered, and the hydrogel volume change could be in principle measured by measuring optical scattering loss.

The combination of covalent and electrostatic bonding of PAM and alginate results in highly elastic and tough hydrogels.[58] Guo et al.[4e] fabricated highly stretchable, tough step-index hydrogel optical fibers using alginate-PAM, which could be axially elongated by 700%. Organic dyes were incorporated into the alginate-PAM fiber, and when stretched, the total optical absorption loss by the dyes increased with the increasing strain. This principle was used to develop strain sensing. Different dyes were doped at different locations along the length of the fiber, allowing distributed strain sensing along the fiber (Figure 6h–j).

Surface plasmon resonance immunoassay[59] is a promising label-free spectroscopic approach for real-time biosensing. Surface plasmon sensors were integrated into hydrogel waveguides.[60] Knoll et al.[61] demonstrated a variety of hydrogel waveguide-based plasmonic sensors.[61] Zourob and Goddard[62] fabricated a plasmonic sensor with a waveguiding layer made of silica sol–gel and agarose hydrogel, which incorporated immobilized glucose oxidase enzymes and antibodies for analyte detection. Pasche et al.[63] demonstrated a wearable hydrogel plasmonic sensor detecting C-reactive protein for monitoring of patient's wound healing. Hong et al.[64] demonstrated hydrogel-coated grating waveguides for detecting specific biochemical ligands.

3.3. Synthetic Bioabsorbable Polymers

Soft biomaterials tend to change their properties over time due to material aging and also interactions with the environment. Hydrolysis and enzymatic reaction are major biodegradation processes in vivo. The speed of biodegradation depends

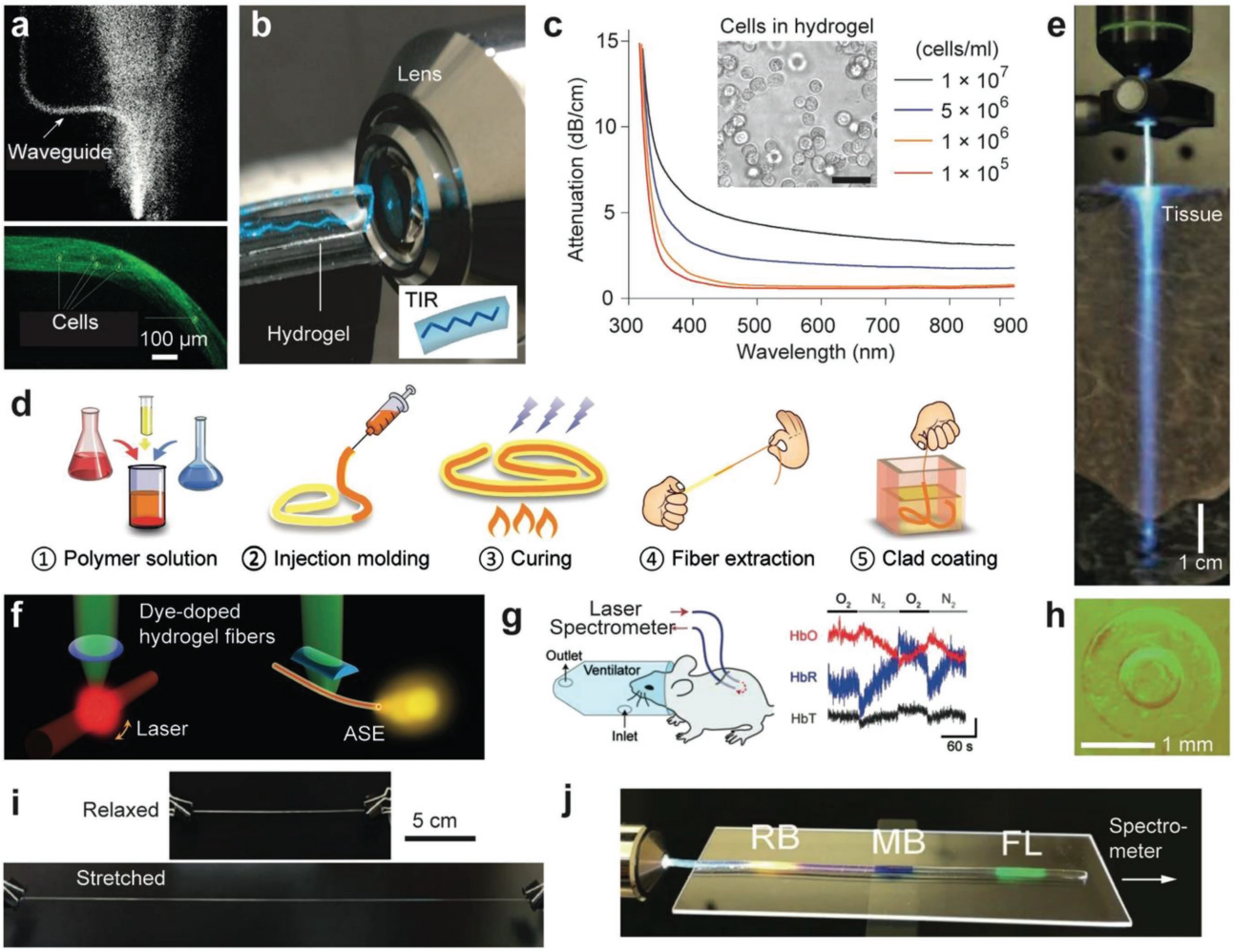

Figure 6. Hydrogel-based optical waveguides. a) Agarose-gel waveguides containing cells.[51] b) Demonstration of total internal reflection in a slab PEG hydrogel.[4g] c) Optical attenuation in PEG hydrogel waveguides containing cells at different concentrations.[4g] d) A fabrication method of core-clad hydrogel fibers.[4h] e) An implanted hydrogel optical fiber in a tissue.[4h] Light leakage along the fiber is seen. f) Optically pumped, dye-doped hydrogel waveguides for generating WGM-type lasing (left) and amplified spontaneous emission (right).[4h] g) Demonstration of in vivo continuous measurement of oxygenated and deoxygenated hemoglobin concentrations using a pair of implanted hydrogel optical fibers.[4h] h) Cross-section images of step-index alginate-PAM hydrogel optical fibers.[4e] i) High stretchability of an alginate-PAM hydrogel optical fiber.[4e] j) A hydrogel fiber doped with three different organic dyes, rose Bengal (RB), methylene blue (MB), and fluorescein (FL), for axial strain sensing.[4e] Figure reproduced with permission from: (a) ref. [51], Copyright 2012, Optical Society of America; (b) and (c) ref. [4g], Copyright 2013, Nature Publishing Group; (e) and (g) ref. [4h], Copyright 2015, Wiley; (h), (i) and (j) ref. [4e], Copyright 2016, Wiley.

on the type of polymers and surface conditions. However, some biomaterials, such as PEG, are relatively bioinert and could provide a long functional lifetime. On the other hands, biodegradable materials can be judiciously used to build implantable devices. These biodegradable devices remain functional during an intended period of operation but, after that, further degrade and eventually are absorbed in the body. Therefore, they do not need to be removed from the body after use by human intervention. For instance, surgical suture threads are made of synthetic biodegradable polymers. Among various biodegradable polymers, the group of polylactic acid (PLA), polyglycolic acid (PGA), and poly(lactic-co-glycolic) acid (PLGA) have received most attention for drug delivery and tissue engineering applications.[65] Different forms of PLGA can be obtained depending on the ratio of lactide to glycolide (e.g. PLGA 75:25 refers to a copolymer with 75% lactic acid and 25% glycolic acid). In general, the biodegradation speed of PLGA increases with decreasing glycolide unit content. PLGA 50:50 exhibits a biodegradation half-life of a few weeks to months depending on the device size. The degraded monomers are resorbable in the body. The enantiomeric forms of PLA are PDLA, PLLA, and PDLLA, in which the ratio of D to L determines the degree of crystallinity. In general, PGA has a higher degree of crystallinity than PDLA or PLLA due to absence of any methyl side groups. The flexibility and rigidity of the polymers can be tuned by controlling polymer molecular weight, degree of crosslinking, functional group modification, and additional monomer blending.

Various biodegradable polymers have been employed to form implantable photonic devices. Choi et al.[66] proposed a

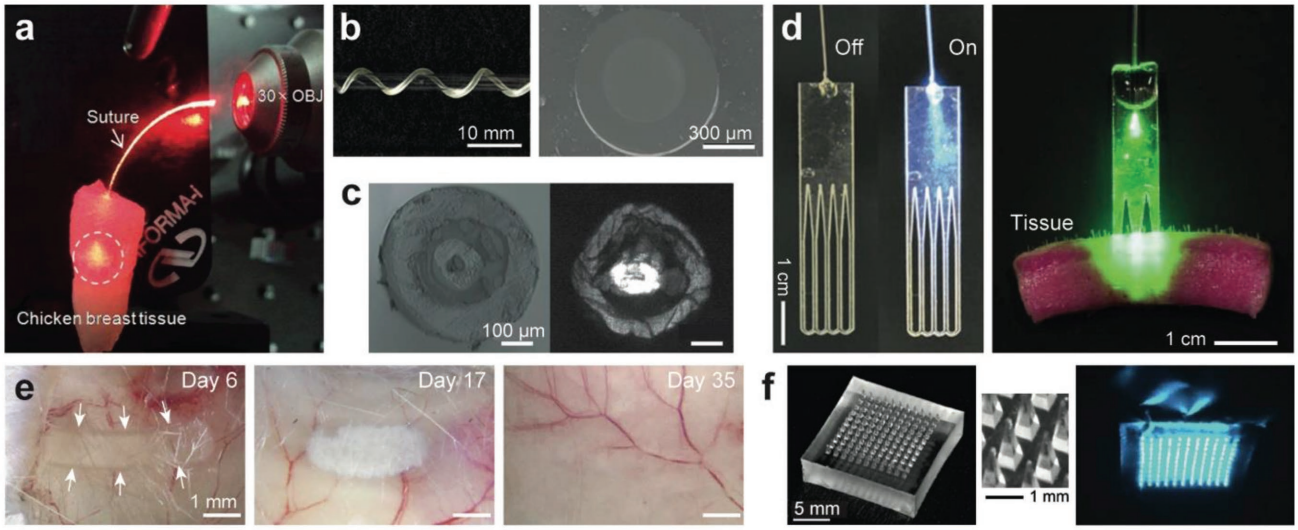

Figure 7. Optical waveguides made from biodegradable polymers. a) A biodegradable PGA surgical suture thread delivering light into a tissue.[66] b) Side-view and cross-section of a POMC-POC optical fiber.[67] c) Cross-section of a multifunctional biodegradable cellulose optical fiber with a central microchannel and a ring core for guiding light.[68a] d) Comb-shape PLLA waveguides designed to deliver photochemical activation light into a thick skin tissue.[4b] e) Time-lapse images showing the biodegradation of a PLA optical waveguide implanted in a subcutaneous region of a mouse.[4b] f) A PLA microneedle array developed for percutaneous light delivery.[69] Figure reproduced with permission from: (a) ref. [66], Copyright 2014, SPIE; (b) ref. [67], Copyright 2017, Wiley; (c) ref. [68a], Copyright 2007, Optical Society of America; (d) and (e) ref. [4b], Nature Publishing Group; (f) ref. [69], Copyright 2016, Optical Society of America.

400-μm-thick surgical suture thread made of PGA, which served as an optical waveguide delivering light for a few centimeters into the tissue (**Figure 7**a). Biodegradable citrate-based step-index optical fibers exhibited controllable optomechanobiological properties and a propagation loss of 0.4 dB cm^{-1}, and showed potential for deep-tissue light delivery and collection (Figure 7b).[67] Using biodegradable cellulose butyrate, Dupuis et al.[68] made double-cladding microstructured optical fibers with a transmission loss of ≈1 dB cm^{-1} (Figure 7c). Nizamoglu et al.[4b] developed a flexible bio-absorbable PLLA optical waveguide comb (Figure 7d) and investigated its potential application to photochemical tissue bonding (PTB). PTB uses a dye and activation light to induce photo-crosslinking between collagen fibers present in tissues for suture-less bonding between tissues. Conventional PTB is applicable to only shallow wounds (<2–3 mm deep cut) due to limited optical penetration into tissues. Nizamoglue et al. inserted the biodegradable PLA waveguide into a full-thickness cut in the porcine skin. The waveguide delivered activation light uniformly over the tissue interface and produced considerably improved tissue bonding strength compared to conventional PTB performed without a waveguide. Biodegradability is critical for this application because the waveguide can be left in the crosslinked tissue and gradually bioabsorbed over time (Figure 7e). Kim et al.[69] developed a PLA microneedle array suitable for cutaneous light delivery (Figure 7f).

Chitosan, a natural biodegradable polymer, has been used for nanocomposite films.[70] Using the property of chitosan films to absorb and release water vapor and gas molecules in the environment, Chen et al. and Voznesenskiya et al.[71] developed chitosan-based fiber-optic humidity sensors. Mironenko et al.[72] controlled the RI of a chitosan thin film by in situ reduction of preabsorbed silver ions in the film. Chitosan composite films containing metallic nanoparticles can have a high RI tunable from 1.53 to 1.69 depending on the metallic dopant concentration. Chitosan/Ag and chitosan/Au composite planar optical waveguides have been developed for hydrogen sulfide gas sensing.[73]

3.4. Elastomers

The mechanical properties, such as elasticity and tensile strength, of optical waveguides are an important specification for biomedical applications. When used in implantable and wearable devices, too stiff materials may break and cause damages to the tissues. Although hydrogels can satisfy the mechanical requirement by offering mechanical moduli similar to those of soft tissues, hydrogels are typically designed to operate in fully swollen wet conditions, and as they lose water, the mechanical and optical characteristics can degrade, and eventually the dried polymer can become stiff and brittle. For proper operations in nonwet environments, various elastic polymers, or elastomers, have been investigated as biomedical optical materials.

Polydimethylsiloxane (PDMS) is a representative elastomeric biomaterial. PDMS is bioinert and nontoxic and have good optical clarity. Stretchable PDMS optical waveguides with a propagation loss of 0.3–0.5 dB cm^{-1} at visible wavelengths have been developed for flexible optical links to laser sources.[74] Kwok et al.[4c] developed a bendable PDMS optical waveguide for uniform illumination on the sclera around the eye globe. A gold-coated PDMS optical waveguide was developed for the motion detection of the human body,[75] in which strain generated microcracks within a reflective gold layer and increased optical transmission loss, allowing the magnitude of strain to be monitored by measuring the loss (**Figure 8**a). A strain sensor using

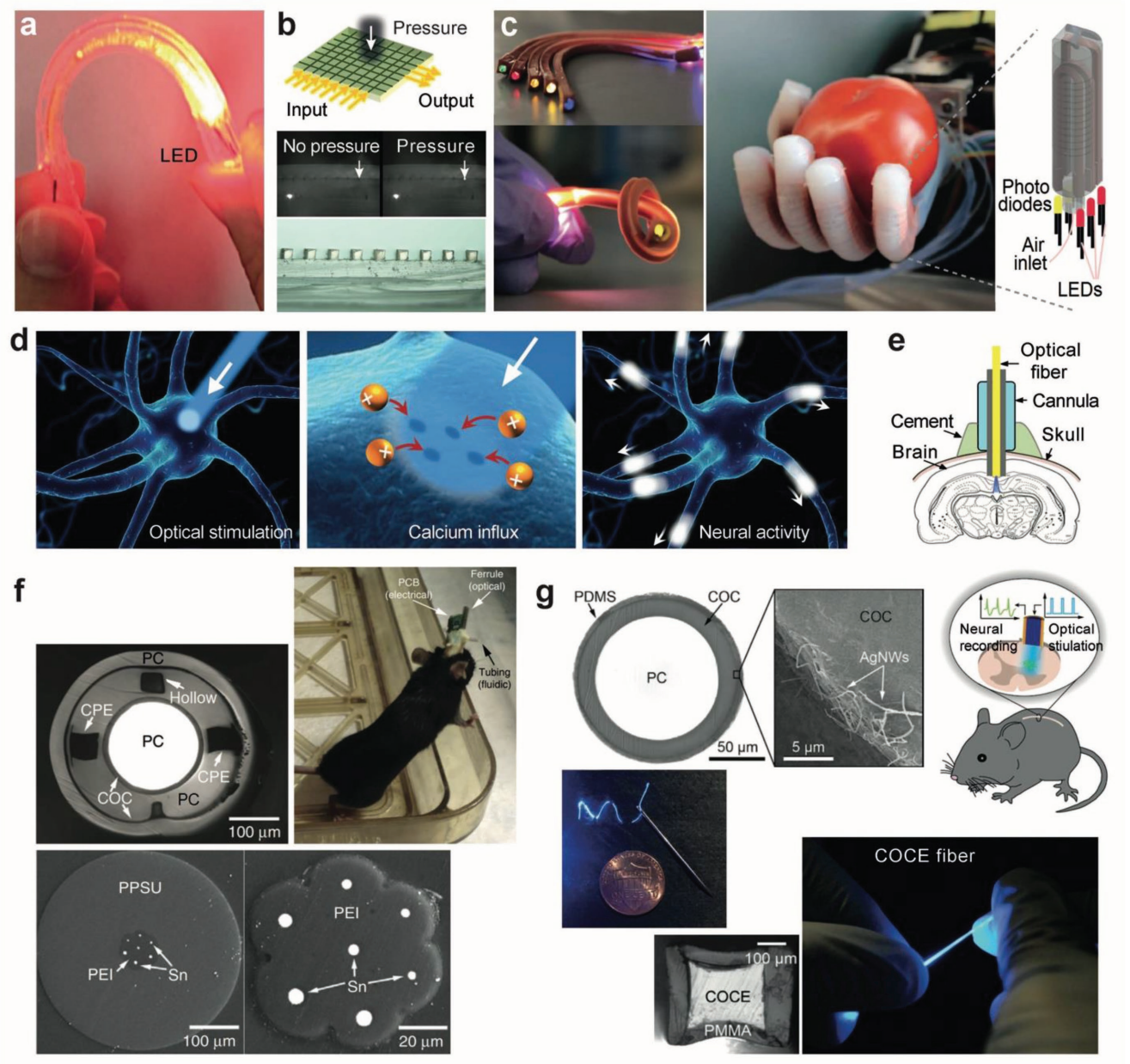

Figure 8. Stretchable and flexible optical waveguides made from elastomeric polymers. a) A gold-coated PDMS optical waveguide sensitive to applied pressure, strain, and bending.[75] b) Crossed PDMS waveguide arrays for artificial skin sensitive to local pressure.[80] c) Optical waveguide made of a polyurethane rubber core and PDMS cladding used in a prosthesis hand capable of sensing the shape and softness of an object.[81] d) Illustration of an optogenetic process: light can open or close genetically engineered ion channels on specific neurons to activate or inhibit neuronal signaling. e) A typical setup to perform optogenetic experiment in deep brain using a rigid optical fiber.[82] f) Polymer-based, multifunctional fibers for simultaneous optical, electrical, and chemical interrogation of neural circuits.[85] g) Flexible and stretchable PMMA-COCE optical fibers for optogenetic stimulation of spinal cords.[86] Figure reproduced with permission from: (a) ref. [75], Copyright 2015, IEEE; (b) ref. [80], Copyright 2009, SPIE; (c) ref. [81], The Copyright 2016, American Association for the Advancement of Science; (e) ref. [82], Copyright 2014, IEEE; (f) ref. [85], Copyright 2015, Nature Publishing Group; (g) ref. [86], Copyright 2017, AAAS.

a dye-doped PDMS fiber was demonstrated for human motion detection and health monitoring, in which strain increased optical loss due to the absorption of the dye molecules.[76] Kolle et al.[77] fabricated a hollow bandgap fiber by rolling PDMS and polyisoprene-polystyrene triblock copolymer (PSPI), a thermoplastic elastomer, films with a RI contrast of 0.13 between the two layers. The concentric layered waveguides were stretchable up to 200%. Upon elongation, the layer thicknesses decreased, and the photonic bandgap spectrum of the multilayer structure were tuned accordingly. PDMS optical waveguide tapers were fabricated via locally stretching and curing PDMS liquid and tested for strain sensing[78] and for optical airflow

sensing.[79] Missinne et al.[80] devised a flat pressure sensor using crossing polymer waveguide arrays within a PDMS matrix. A localized force changes the distance between the two individual crossing waveguides and affects the light coupling between the waveguides, which can be optically measured (Figure 8b). Zhao et al.[81] developed an optical waveguide consisting of a transparent polyurethane rubber core and a highly absorptive silicone composite cladding and introduced the waveguide into a robotic hand for optical haptic sensors (Figure 8c).

Optogenetic techniques based on light-sensitive channel rhodopsins allow the control of neuronal signals by light (Figure 8d). Silica-based optical fibers (Figure 8e)[82] and microfabricated waveguide arrays[83] have been applied to access the brain of live mice in optogenetic experiments. The shear moduli of the glass and plastic fibers are as high as a few GPa, whereas the shear moduli of brain tissues and spinal cords are in the range of 10–300 kPa.[84] The large mismatch in mechanical stiffness poses significant challenges to protect the tissues from being damaged by the implanted waveguides. To solve this problem, Canales et al.[85] developed polymeric multifunctional fibers that provided simultaneous optical stimulation, neural recording, and microfluidic drug delivery over two months in vivo (Figure 8f). Lu et al.[86] reported a flexible and stretchable optical fibers using a cyclic olefin copolymer elastomer core and PDMS cladding that is coated with a thin conductive layer of silver nanowires for recording neuronal electric signals from spinal cords (Figure 8g). The fiber had a shear modulus of about 10 MPa, two orders of magnitude lower than conventional optical fibers and was highly stretchable up to twice the original length. The optical loss of the fiber was relatively high (≈4 dB cm^{-1}) but improved to 1.9 dB cm^{-1} when a stiffer polycarbonate polymer was used for the core.

4. Biomedical Applications

We have reviewed the recent progress in optical biomaterials and waveguides made from them. Some of the waveguide devices are in early conceptual stages, but others are more advanced and have shown a promising feasibility for biomedical applications. Further advances in both the material and device levels are fully expected, and efforts to translate successful technologies to the clinic will follow. Certainly, the introduction of light-guiding biomaterials has opened the door to novel wearable, implantable, injectable optical waveguides, and waveguide-integrated biophotonic devices for a broad range of applications from sensing and diagnosis to drug delivery to phototherapy (**Figure 9**). Here we discuss some examples of the anticipated applications.

4.1. Continuous Sensing Inside the Body

A wide range of fluorescent and luminescent probes are available and have been used in hospital pathology labs to examine tissue slices, blood samples, and cells harvested from tissues. These probes include antibody-conjugated organic dyes against target proteins and biomarkers, dye-conjugated nucleic acids for detecting specific gene expression levels, PH-sensitive fluorophores, and Förster resonance energy transfer fluorescence sensors. Almost all of these standard probes can be incorporated into implantable, transparent light-guiding hydrogels (Figure 9a) and can be fiber-optically accessed from outside the body. This approach allows continuous monitoring of certain proteins, peptides, RNAs, and electrolytes and detection of biomarkers and toxic substances in vivo. This continuous sensing approach requires the implantation of the hydrogel sensors. Although this invasive procedure may not be readily acceptable for healthy individuals, patients who have medical problems may be more receptive to having a personalized implant tailored for the specific medical conditions of the patient.

4.2. Post-Surgical Monitoring of Tissues In Situ

Another potential role of optical waveguide implants is post-surgery monitoring of a patient. For example, for a patient receiving organ transplantation, a pair of optical fibers or a 2D mesh-type waveguide device may be placed near the grafted organ during the transplantation operation (Figure 9b). Various physiological conditions, such as blood perfusion, oxygen consumption, and tissue viability, in the grafted organ can in principle be monitored by performing label-free optical spectroscopy by the implanted waveguide.[4h] In addition, specific fluorescence probes may be embedded in the waveguide to complement label-free sensing. Another example is post-operative monitoring of patient's condition, recovery, or rehabilitation. In all these cases, biodegradable materials would be appropriate so that implanted waveguides are absorbed and disappear over time without needing to surgically remove them afterwards.

4.3. Phototherapies and Optogenetic Treatments

Phototherapies, such as blue light therapy, photodynamic therapy (PDT), and photobiomodulation, are established treatment modalities in the clinic.[1] However, light attenuation in tissues limits the maximum therapeutic depths to several millimeters. A needle-type waveguide may be used to deliver light into deeper target tissues. This minimally invasive approach may be adopted most easily in dermatologic applications, for example, to treat nonmelanoma skin cancer. Currently, PDT is effective only for small tumors located at a shallow depth below the skin surface. Percutaneous light delivery using an optical microneedle array may enable PDT to be applicable to larger and deeper tumors (Figure 9c).[69]

Photochemical crosslinking is a clinical procedure to treat keratoconus and corneal ectasia. Similar to PTB, corneal crosslinking uses riboflavin and light to activate photosensitizers, such as riboflavin, to induce crosslinking in the collagen-rich corneal stroma. This improves the mechanical properties of the corneal tissue and promotes collagen fiber regeneration. A similar procedure on the sclera has been proposed for the treatment of myopia. The underlying idea is to stiffen the sclera to impede the growth of the eye globe during childhood and, thereby, to prevent excessive eye lengthening associated with pathologic myopia. While the biological effects and efficacy of

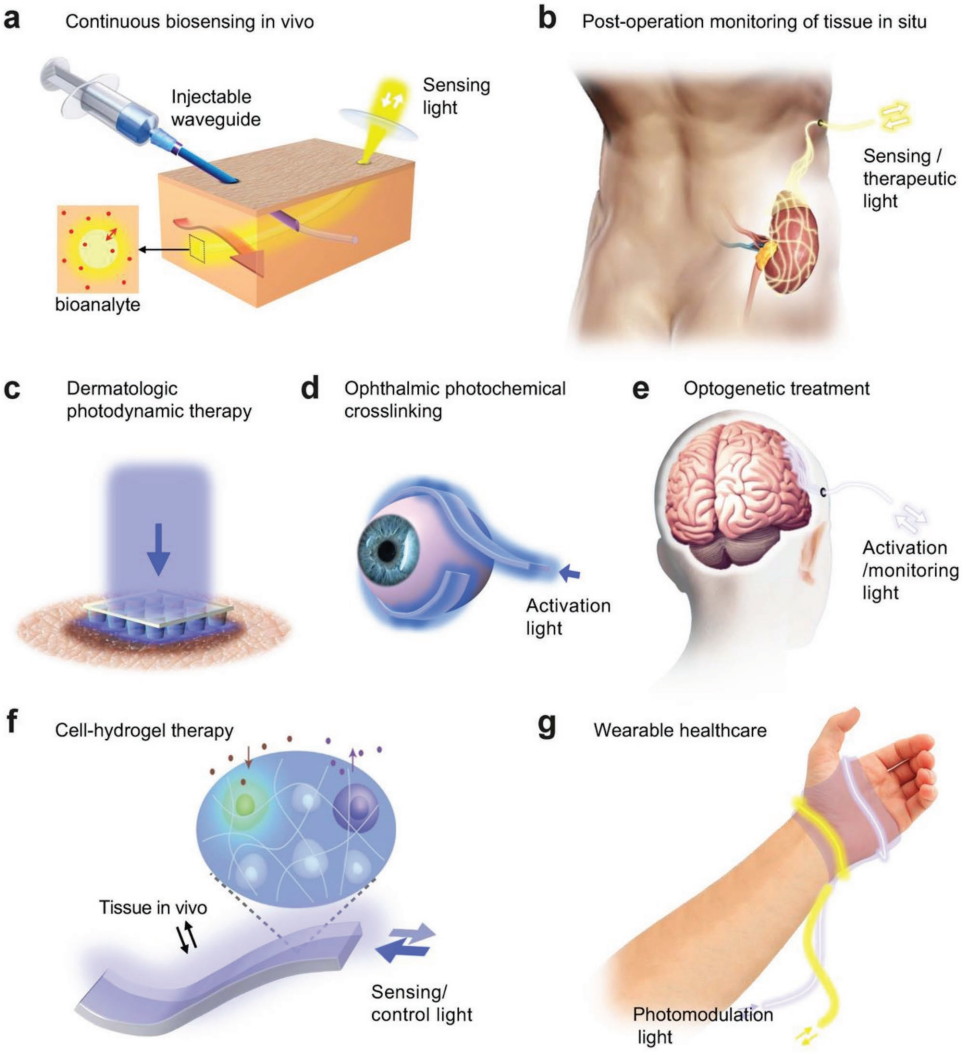

Figure 9. Potential medical applications of biomaterial waveguides. a) Continuous monitoring of biological analytes using an implanted optical fiber. b) Monitoring of the viability and function of a transplanted kidney using a mesh-type optical waveguide. c) Photodynamic therapy of skin tumors using an optical microneedle array. d) Minimally invasive photochemical crosslinking of the sclera using a flexible waveguide. e) Long-term optogenetic treatment of brain disorders using implanted optical waveguides. f) On-demand synthesis of therapeutic substances from optogenetic cells encapsulated in a light-guiding hydrogel implant. g) Photomodulation of wound healing using a wearable photonic bandage.

this proposed technique have yet to be understood, practically scleral crosslinking poses a challenge in delivering light to the scleral tissues around the eye globe. For this purpose, flexible elastomer optical waveguides may be used (Figure 9d). With a proper waveguide design, the magnitude and uniformity of light extraction to the sclera can be optimized while light leakage to the surrounding extraocular tissues is minimized.

Optogenetics is currently a research tool requiring a safe and efficient gene transfection of specifically targeted cells. Significant efforts are being made to translate this power technique to the clinic for the treatment of degenerative brain disorders, spinal injuries, and other neurological problems. Elastically flexible optical waveguides can provide an attractive option for delivering therapeutic light to target regions in the brain and spinal cords. Biomaterial fibers may be injected via a minimally-invasive procedure. For cases when a surgical procedure is necessary for other reasons such as optogenetic gene transfection, biodegradable optical fibers or an optical mesh waveguide with a custom shape may be implanted during the surgery (Figure 9e).

Besides channel rhodopsins, various other light-sensitive proteins and light-sensing domains may be incorporated into cells for light-controlled gene expression. This technique has a potential in cell therapy and gene therapy with an advantage that the therapeutic process can be controlled and monitored optically. In this case, biomaterial optical waveguides can serve as a communication channel between the genetically modified cells and an external control device. Furthermore, light-guiding hydrogels can encapsulate optogenetically engineered cells in their porous polymer network or in embedded microfluidic channels, providing adequate physiological and biophysical, as well as optical, environment (Figure 9f).

4.4. Wearable Optical Devices

Wearable healthcare devices are of great interest for real-time monitoring of individuals during normal life outside hospital settings. The devices can collect longitudinal data over time to assess the health of the individuals. For patients, such devices may assist to evaluate the progression of disease and detect life-threatening conditions and generate alarm signals. Together with various electronics options,[87] optical sensing[88] using integrated waveguides and fiber-optic connection to an external portable device is an attractive option as it does not require electrical power within the wearables, is free from electromagnetic interference and lightweight, and can utilize various luminescent chemical and biological probes. Optical wearables can also incorporate therapeutics such as photobiomodulation. For example, one may imagine a photonic bandage (Figure 9g) that is wrapped around a wounded area, measuring temperature using temperature-sensitive fluorescent probes, monitoring oxygen perfusion using diffuse spectroscopy, and infusing near-infrared light into the wound to relieve pain and promote healing.

Acknowledgements

S.S. and S.K. contributed equally to this work. The authors thank Sheldon J.J. Kwok and Behrouz Tavakol for discussions and Sarah Forward for assistance in preparing the manuscript. This work was funded by the U.S. Air Force Office of Scientific Research (AFOSR; grant FA9550-17-1-0277), National Institutes of Health (NIH, grants R01CA192878, P41 EB015903), and the Korea Institute of Science and Technology (KIST).

Conflict of Interest

The authors declare no conflict of interest.

Keywords

biocompatible optical materials, biodegradable waveguides, biophotonic waveguides, elastic waveguides

Received: November 14, 2017
Revised: January 16, 2018
Published online:

[1] S. H. Yun, S. J. J. Kwok, *Nat. Biomed. Eng.* **2017**, *1*, 0008.
[2] S. Shabahang, F. A. Tan, J. D. Perlstein, G. Tao, O. Alvarez, F. Chenard, A. Sincore, L. Shah, M. C. Richardson, K. L. Schepler, A. F. Abouraddy, *Opt. Mater. Express* **2017**, *7*, 2336.
[3] B. Temelkuran, S. D. Hart, G. Benoit, J. D. Joannopoulos, Y. Fink, *Nature* **2002**, *420*, 650.
[4] a) S. Nizamoglu, M. C. Gather, S. H. Yun, *Adv. Mater.* **2013**, *25*, 5943; b) S. Nizamoglu, M. C. Gather, M. Humar, M. Choi, S. Kim, K. S. Kim, S. K. Hahn, G. Scarcelli, M. Randolph, R. W. Redmond, S. H. Yun, *Nat. Commun.* **2016**, *7*, 10374; c) S. J. J. Kwok, M. Kim, H. H. Lin, T. G. Seiler, E. Beck, P. Shao, I. E. Kochevar, T. Seiler, S.-H. Yun, *Invest. Ophthalmol. Visual Sci.* **2017**, *58*, 2596; d) A. K. Yetisen, N. Jiang, A. Fallahi, Y. Montelongo, G. U. Ruiz-Esparza, A. Tamayol, Y. S. Zhang, I. Mahmood, S. A. Yang, K. S. Kim, H. Butt, A. Khademhosseini, S. H. Yun, *Adv Mater.* **2017**, *29*, 1606380; e) J. Guo, X. Liu, N. Jiang, A. K. Yetisen, H. Yuk, C. Yang, A. Khademhosseini, X. Zhao, S. H. Yun, *Adv. Mater.* **2016**, *28*, 10244; f) M. Humar, S. H. Yun, *Nat. Photonics* **2015**, *9*, 572; g) M. Choi, J. W. Choi, S. Kim, S. Nizamoglu, S. K. Hahn, S. H. Yun, *Nat. Photonics* **2013**, *7*, 987; h) M. Choi, M. Humar, S. Kim, S. H. Yun, *Adv. Mater.* **2015**, *27*, 4081; i) M. Humar, S. H. Yun, *Optica* **2017**, *4*, 222.
[5] M. Jacobs, M. Lopez-Garcia, O.-P. Phrathep, T. Lawson, R. Oulton, H. M. Whitney, *Nat. Plants* **2016**, *2*, 16162.
[6] D. Attenborough, *The Private Life of Plants: A Natural History of Plant Behaviour*, Princeton University Press, Princeton, NJ, USA **1995**.
[7] C. R. Brodersen, T. C. Vogelmann, *Am. J. Bot.* **2007**, *94*, 1061.
[8] G. Karabourniotis, *J. Exp. Bot.* **1998**, *49*, 739.
[9] S. Hammer, *Lithops: Joyaux du veld* Quae éditions, Versailles, France **2010**.
[10] D. F. Mandoli, W. R. Briggs, *Sci. Am.* **1984**, *251*, 90.
[11] a) M. Mo, K. Yokawa, Y. Wan, F. Baluška, *Front. Plant Sci.* **2015**, *6*, 775; b) C. Galen, J. J. Rabenold, E. Liscum, *Plant Signal. Behav.* **2007**, *2*, 106.
[12] a) Q. Sun, K. Yoda, M. Suzuki, H. Suzuki, *J. Exp. Bot.* **2003**, *54*, 1627; b) Q. Sun, K. Yoda, H. Suzuki, *J. Exp. Bot.* **2004**, *56*, 191.
[13] H.-J. Lee, J.-H. Ha, S.-G. Kim, H.-K. Choi, Z. H. Kim, Y.-J. Han, J.-I. Kim, Y. Oh, V. Fragoso, K. Shin, *Sci. Signal.* **2016**, *9*, ra106.
[14] a) H. J. Hoving, L. D. Zeidberg, M. C. Benfield, S. L. Bush, B. H. Robison, M. Vecchione, *Proc. Biol. Sci.* **2013**, *280*, 20131463; b) E. A. Widder, *Environ. Biol. Fishes* **1998**, *53*, 267; c) P. Herring, *The Biology of the Deep Ocean*, Oxford University Press, Oxford **2001**; d) M. Miya, T. W. Pietsch, J. W. Orr, R. J. Arnold, T. P. Satoh, A. M. Shedlock, H.-C. Ho, M. Shimazaki, M. Yabe, M. Nishida, *BMC Evol. Biol.* **2010**, *10*, 58; e) S. H. Haddock, C. W. Dunn, P. R. Pugh, C. E. Schnitzler, *Science* **2005**, *309*, 263.
[15] Y. P. Hsieh, J. Rudloe, *Trends Food Sci. Technol.* **1994**, *5*, 225.
[16] M. Zimmer, *Glowing Genes: A Revolution in Biotechnology*, Prometheus Books, Amherst, NY, USA **2005**.
[17] A. W. Snyder, in *Comparative Physiology and Evolution of Vision in Invertebrates: A: Invertebrate Photoreceptors*, (Eds: H. Autrum, M. F. Bennett, B. Diehn, K. Hamdorf, M. Heisenberg, M. Järvilehto, P. Kunze, R. Menzel, W. H. Miller, A. W. Snyder, D. G. Stavenga, M. Yoshida, H. Autrum), Springer, Berlin **1979**, p. 225.
[18] a) M. F. Land, D.-E. Nilsson, *Animal Eyes*, Oxford University Press, Oxford, England, UK **2012**; b) M. F. Land, *Annu. Rev. Entomol.* **1997**, *42*, 147.
[19] E. Newman, A. Reichenbach, *Trends Neurosci.* **1996**, *19*, 307.
[20] a) K. Franze, J. Grosche, S. N. Skatchkov, S. Schinkinger, C. Foja, D. Schild, O. Uckermann, K. Travis, A. Reichenbach, J. Guck, *Proc. Natl. Acad. Sci. USA* **2007**, *104*, 8287; b) S. Agte, S. Junek, S. Matthias, E. Ulbricht, I. Erdmann, A. Wurm, D. Schild, J. A. Kas, A. Reichenbach, *Biophys. J.* **2011**, *101*, 2611.
[21] A. M. Labin, S. K. Safuri, E. N. Ribak, I. Perlman, *Nat. Commun.* **2014**, *5*, 4319.
[22] D. Colladon, *Comptes Rendus* **1842**, *15*, 800.
[23] J. Hecht, *City of Light: The Story of Fiber Optics*, Oxford University Press on Demand, Oxford, England, UK **2004**.
[24] J. Tyndall, *Notes about Light*, William & Sons **1870**.
[25] A. Lepère, É. Monod, *The illuminated fountains Auguste Lepère,* Paris world fair, Paris **1889**.
[26] W. Wheeler, *U.S. Patent 247,229*, **1881**.
[27] M. H. Knisely, *Anat. Rec.* **1936**, *64*, 499.
[28] J. L. Meikle, *American Plastic: A Cultural History*, Rutgers University Press, **1995**.
[29] R. J. Brown, *Popular Sci.* **1939**, March, 108.
[30] H. Osterberg, E. Snitzer, M. Polanyi, R. Hilberg, J. Hicks, *J. Opt. Soc. Am.* **1959**, *49*, 1128.
[31] G. J. Goubau, *US Patent 2, 994, 873*, **1961**.
[32] M. Jones, K. Kao, *J. Phys. E: Sci. Instrum.* **1969**, *2*, 331.

[33] a) A. Mekis, S. Fan, J. D. Joannopoulos, *Phys. Rev. B* **1998**, *58*, 4809; b) J. C. Knight, J. Broeng, T. A. Birks, P. S. J. Russell, *Science* **1998**, *282*, 1476.
[34] a) J. J. Kaufman, G. Tao, S. Shabahang, D. S. Deng, Y. Fink, A. F. Abouraddy, *Nano Lett.* **2011**, *11*, 4768; b) S. Shabahang, G. Tao, J. J. Kaufman, Y. Qiao, L. Wei, T. Bouchenot, A. P. Gordon, Y. Fink, Y. Bai, R. S. Hoy, *Nature* **2016**, *534*, 529; c) G. Tao, J. J. Kaufman, S. Shabahang, R. R. Naraghi, S. V. Sukhov, J. D. Joannopoulos, Y. Fink, A. Dogariu, A. F. Abouraddy, *Proc. Natl. Acad. Sci. USA* **2016**, *113*, 6839.
[35] C. P. Bergmann, A. Stumpf, in *Dental Ceramics: Microstructure, Properties and Degradation*, https://doi.org/10.1007/978-3-642-38224-6_2 (Eds: C. Bergmann, A. Stumpf), Springer, Berlin **2013**, p. 9.
[36] D. F. Williams, *Definitions in Biomaterials: Proc. of a Consensus Conf. of the Eur. Soc. for Biomaterials, Chester, England, March 3–5, 1986*, Elsevier Science Limited, **1987**.
[37] S. L. Jacques, *Phys. Med. Biol.* **2013**, *58*, 5007.
[38] A. Bezryadina, T. Hansson, R. Gautam, B. Wetzel, G. Siggins, A. Kalmbach, J. Lamstein, D. Gallardo, E. J. Carpenter, A. Ichimura, *Phys. Rev. Lett.* **2017**, *119*, 058101.
[39] H. Xin, Y. Li, X. Liu, B. Li, *Nano Lett.* **2013**, *13*, 3408.
[40] a) F. G. Omenetto, D. Kaplan, *Nat. Photonics* **2008**, *2*, 641; b) S. T. Parker, P. Domachuk, J. Amsden, J. Bressner, J. A. Lewis, D. L. Kaplan, F. G. Omenetto, *Adv. Mater.* **2009**, *21*, 2411; c) H. Tao, D. L. Kaplan, F. G. Omenetto, *Adv. Mater.* **2012**, *24*, 2824.
[41] B. D. Lawrence, M. Cronin-Golomb, I. Georgakoudi, D. L. Kaplan, F. G. Omenetto, *Biomacromolecules* **2008**, *9*, 1214.
[42] H. Perry, A. Gopinath, D. L. Kaplan, L. Dal Negro, F. G. Omenetto, *Adv. Mater.* **2008**, *20*, 3070.
[43] X. Qiao, Z. Qian, J. Li, H. Sun, Y. Han, X. Xia, J. Zhou, C. Wang, Y. Wang, C. Wang, *ACS Appl. Mater. Interfaces* **2017**, *9*, 14665.
[44] M. B. Applegate, G. Perotto, D. L. Kaplan, F. G. Omenetto, *Biomed. Opt. Express* **2015**, *6*, 4221.
[45] J. P. Mazzoccoli, D. L. Feke, H. Baskaran, P. N. Pintauro, *J. Biomed. Mater. Res., Part A* **2010**, *93*, 558.
[46] a) A. S. Hoffman, *Adv. Drug Delivery Rev.* **2013**, *65*, 10; b) P. Bajaj, R. M. Schweller, A. Khademhosseini, J. L. West, R. Bashir, *Annu. Rev. Biomed. Eng.* **2014**, *16*, 247.
[47] a) J. Li, D. J. Mooney, **2016**, *1*, 16071; b) G. Tiwari, R. Tiwari, B. Sriwastawa, L. Bhati, S. Pandey, P. Pandey, S. K. Bannerjee, *Int. J. Pharm. Invest.* **2012**, *2*, 2; c) M. W. Tibbitt, J. E. Dahlman, R. Langer, *J. Am. Chem. Soc.* **2016**, *138*, 704.
[48] a) H. A. Awad, M. Quinn Wickham, H. A. Leddy, J. M. Gimble, F. Guilak, *Biomaterials* **2004**, *25*, 3211; b) R. L. Mauck, M. A. Soltz, C. C. Wang, D. D. Wong, P.-H. G. Chao, W. B. Valhmu, C. T. Hung, G. A. Ateshian, *J. of Biomech. Eng.* **2000**, *122*, 252; c) K. T. Paige, L. G. Cima, M. J. Yaremchuk, B. L. Schloo, J. P. Vacanti, C. A. Vacanti, *Plast. Reconstr. Surg.* **1996**, *97*, 168.
[49] a) A. G. Mikos, M. G. Papadaki, S. Kouvroukoglou, S. L. Ishaug, R. C. Thomson, *Biotechnol. Bioeng.* **1994**, *43*, 673; b) C. Perka, R. S. Spitzer, K. Lindenhayn, M. Sittinger, O. Schultz, *J. Biomed. Mater. Res., Part A* **2000**, *49*, 305; c) K. Y. Lee, E. Alsberg, D. J. Mooney, *J. Biomed. Mater. Res., Part A* **2001**, *56*, 228; d) K. Y. Lee, D. J. Mooney, *Chem. Rev.* **2001**, *101*, 1869; e) H. Park, B. Choi, J. Hu, M. Lee, *Acta Biomater.* **2013**, *9*, 4779.
[50] A. K. Manocchi, P. Domachuk, F. G. Omenetto, H. Yi, *Biotechnol. Bioeng.* **2009**, *103*, 725.
[51] A. Jain, A. H. Yang, D. Erickson, *Opt. Lett.* **2012**, *37*, 1472.
[52] J. Zhu, *Biomaterials* **2010**, *31*, 4639.
[53] H. Ye, M. D.-E. Baba, R.-W. Peng, M. Fussenegger, *Science* **2011**, *332*, 1565.
[54] W. H. Organization, *Global Report on Diabetes*, World Health Organization, **2016**.
[55] Y. J. Heo, H. Shibata, T. Okitsu, T. Kawanishi, S. Takeuchi, *Proc. Natl. Acad. Sci. USA* **2011**, *108*, 13399.
[56] a) T. Saxl, F. Khan, M. Ferla, D. Birch, J. Pickup, *Analyst* **2011**, *136*, 968; b) T. Peyser, H. Zisser, U. Khan, L. Jovanovic, W. Bevier, M. Romey, J. Suri, P. Strasma, S. Tiaden, S. Gamsey, *J. Diabetes Sci. Technol.* **2011**, *5*, 687.
[57] E. A. Moschou, B. V. Sharma, S. K. Deo, S. Daunert, *J. Fluoresc.* **2004**, *14*, 535.
[58] J.-Y. Sun, X. Zhao, W. R. Illeperuma, O. Chaudhuri, K. H. Oh, D. J. Mooney, J. J. Vlassak, Z. Suo, *Nature* **2012**, *489*, 133.
[59] B. Liedberg, C. Nylander, I. Lunström, *Sens. Actuators* **1983**, *4*, 299.
[60] P. W. Beines, I. Klosterkamp, B. Menges, U. Jonas, W. Knoll, *Langmuir* **2007**, *23*, 2231.
[61] a) W. Knoll, A. Kasry, F. Yu, Y. I. Wang, A. Brunsen, J. DostÁLek, *J. Nonlinear Opt. Phys. Mater.* **2008**, *17*, 121; b) Y. Wang, A. Brunsen, U. Jonas, J. Dostalek, W. Knoll, *Anal. Chem.* **2009**, *81*, 9625; c) Y. Wang, C. J. Huang, U. Jonas, T. Wei, J. Dostalek, W. Knoll, *Biosens. Bioelectron.* **2010**, *25*, 1663; d) C. J. Huang, J. Dostalek, W. Knoll, *Biosens. Bioelectron.* **2010**, *26*, 1425; e) Q. Zhang, Y. Wang, A. Mateescu, K. Sergelen, A. Kibrom, U. Jonas, T. Wei, J. Dostalek, *Talanta* **2013**, *104*, 149.
[62] M. Zourob, N. J. Goddard, *Biosens. Bioelectron.* **2005**, *20*, 1718.
[63] S. Pasche, S. Angeloni, R. Ischer, M. Liley, J. Luprano, G. Voirin, *Adv. Sci. Technol.* **2008**, *57*, 80.
[64] Y. S. Hong, J. Kim, H. K. Sung, *Sensors* **2016**, 16.
[65] a) J. Z. Wu, G. R. Williams, H. Y. Li, D. X. Wang, S. D. Li, L. M. Zhu, *Drug Delivery* **2017**, *24*, 1513; b) M. Alibolandi, F. Alabdollah, F. Sadeghi, M. Mohammadi, K. Abnous, M. Ramezani, F. Hadizadeh, *J. Controlled Release* **2016**, *227*, 58; c) H. Cho, J. Gao, G. S. Kwon, *J. Controlled Release* **2016**, *240*, 191; d) A. M. de Groot, G. Du, J. Monkare, A. C. M. Platteel, F. Broere, J. A. Bouwstra, A. Sijts, *J. Controlled Release* **2017**, *266*, 27; e) G. Du, R. M. Hathout, M. Nasr, M. R. Nejadnik, J. Tu, R. I. Koning, A. J. Koster, B. Slutter, A. Kros, W. Jiskoot, J. A. Bouwstra, J. Monkare, *J. Controlled Release* **2017**, *266*, 109; f) B. Grunwald, J. Vandooren, E. Locatelli, P. Fiten, G. Opdenakker, P. Proost, A. Kruger, J. P. Lellouche, L. L. Israel, L. Shenkman, M. Comes Franchini, *J. Controlled Release* **2016**, *239*, 39.
[66] W. J. Choi, K. S. Park, B. H. Lee, *J. Biomed. Opt.* **2014**, *19*, 3.
[67] D. Shan, C. Zhang, S. Kalaba, N. Mehta, G. B. Kim, Z. Liu, J. Yang, *Biomaterials* **2017**, *143*, 142.
[68] a) A. Dupuis, N. Guo, Y. Gao, N. Godbout, S. Lacroix, C. Dubois, M. Skorobogatiy, *Opt. Lett.* **2007**, *32*, 109; b) P. Kunthadong, R. Molloy, P. Worajittiphon, T. Leejarkpai, N. Kaabbuathong, W. Punyodom, *J. Polym. Environ.* **2015**, *23*, 107.
[69] M. Kim, J. An, K. S. Kim, M. Choi, M. Humar, S. J. Kwok, T. Dai, S. H. Yun, *Biomed. Opt. Express* **2016**, *7*, 4220.
[70] T. D. Rathke, S. M. Hudson, *J. Macromol. Sci., Polym. Rev.* **1994**, *34*, 375.
[71] a) L. H. Chen, T. Li, C. C. Chan, R. Menon, P. Balamurali, M. Shaillender, B. Neu, X. M. Ang, P. Zu, W. C. Wong, K. C. Leong, *Sens. Actuators, B* **2012**, *169*, 167; b) S. S. Voznesenskiy, A. A. Sergeev, A. Y. Mironenko, S. Y. Bratskaya, Y. N. Kulchin, *Sens. Actuators, B* **2013**, *188*, 482.
[72] A. Mironenko, E. Modin, A. Sergeev, S. Voznesenskiy, S. Bratskaya, *Chem. Eng. J* **2014**, *244*, 457.
[73] A. Y. Mironenko, A. A. Sergeev, A. E. Nazirov, E. B. Modin, S. S. Voznesenskiy, S. Y. Bratskaya, *Sens. Actuators, B* **2016**, *225*, 348.
[74] a) I. Martincek, D. Pudis, M. Chalupova, *IEEE Photonics Technol. Lett.* **2014**, *26*, 1446; b) J. Missinne, S. Kalathimekkad, B. Van Hoe, E. Bosman, J. Vanfleteren, G. Van Steenberge, *Optics Express* **2014**, *22*, 4168.
[75] C. To, T. L. Hellebrekers, Y.-L. Park, presented at *Intelligent Robots and Systems (IROS)*, Hamburg, Germany, September **2015**.
[76] J. Guo, M. Niu, C. Yang, *Optica* **2017**, *4*, 1285.
[77] M. Kolle, A. Lethbridge, M. Kreysing, J. J. Baumberg, J. Aizenberg, P. Vukusic, *Adv. Mater.* **2013**, *25*, 2239.

[78] I. Martincek, D. Pudis, P. Gaso, *IEEE Photonics Technol. Lett.* **2013**, *25*, 2066.
[79] J. Paek, J. Kim, *Nat. Commun.* **2014**, 5.
[80] J. Missinne, G. Van Steenberge, B. Van Hoe, K. Van Coillie, T. Van Gijseghem, P. Dubruel, J. Vanfleteren, P. Van Daele, *presented at SPIE OPTO: Integrated Optoelectronic Devices* San Jose, California, United States, February 2009.
[81] H. Zhao, K. O'Brien, S. Li, R. F. Shepherd, *Science Robotics* **2016**, *1*, eaai7529.
[82] R. Pashaie, P. Anikeeva, J. H. Lee, R. Prakash, O. Yizhar, M. Prigge, D. Chander, T. J. Richner, J. Williams, *IEEE Rev. Biomed. Eng.* **2014**, *7*, 3.
[83] A. N. Zorzos, J. Scholvin, E. S. Boyden, C. G. Fonstad, *Opt. Lett.* **2012**, *37*, 4841.
[84] S. Cheng, E. C. Clarke, L. E. Bilston, *Med. Eng. Phys.* **2008**, *30*, 1318.
[85] A. Canales, X. Jia, U. P. Froriep, R. A. Koppes, C. M. Tringides, J. Selvidge, C. Lu, C. Hou, L. Wei, Y. Fink, *Nat. Biotechnol.* **2015**, 33.
[86] C. Lu, S. Park, T. J. Richner, A. Derry, I. Brown, C. Hou, S. Rao, J. Kang, C. T. Moritz, Y. Fink, *Sci. Adv.* **2017**, *3*, e1600955.
[87] a) V. Lumelsky, M. S. Shur, S. Wagner, *Sensitive Skin*, World Scientific, River Edge, NJ, USA **2000**; b) T. Someya, T. Sekitani, S. Iba, Y. Kato, H. Kawaguchi, T. Sakurai, *Proc. Natl. Acad. Sci USA* **2004**, *101*, 9966; c) V. Maheshwari, R. Saraf, *Angew. Chem., Int. Ed.* **2008**, *47*, 7808.
[88] M. Ramuz, B. C. K. Tee, J. B. H. Tok, Z. Bao, *Adv. Mater.* **2012**, *24*, 3223.
[89] C. M. Torres, *Ann. Mus. civ. Rovereto Sez.: Arch., St., Sc. nat.* **2014**, *29*, 219.
[90] S. H. D. Haddock, M. A. Moline, J. F. Case, *Annu. Rev. Mar. Sci.* **2010**, *2*, 443.
[91] S. Schwarz, A. Narendra, J. Zeil, *Arthropod Struct. Dev.* **2011**, *40*, 128.
[92] D. Colladon, *La Nature* **1884**, *12*, 325.
[93] N. Huby, V. Vié, A. Renault, S. Beaufils, T. Lefèvre, F. Paquet-Mercier, M. Pézolet, B. Bêche, *Appl. Phys. Lett.* **2013**, *102*, 123702.
[94] a) S. Kujala, A. Mannila, L. Karvonen, K. Kieu, Z. Sun, *Sci. Rep.* **2016**, *6*, 22358; b) H.-Y. Cheung, K.-T. Lau, M.-P. Ho, A. Mosallam, *J. Compos. Mater.* **2009**, *43*, 2521; c) J. Pérez-Rigueiro, C. Viney, J. Llorca, M. Elices, *J. Appl. Polym. Sci.* **2000**, *75*, 1270; d) Q. Lu, B. Zhang, M. Li, B. Zuo, D. L. Kaplan, Y. Huang, H. Zhu, *Biomacromolecules* **2011**, *12*, 1080; e) Y. Cao, B. Wang, *Int. J. Mol. Sci.* **2009**, *10*, 1514.
[95] a) C. Vepari, D. L. Kaplan, *Prog. Polym. Sci.* **2007**, *32*, 991; b) M. Elices, G. V. Guinea, J. Pérez-Rigueiro, G. R. Plaza, *JOM* **2005**, *57*, 60; c) F. Vollrath, P. Barth, A. Basedow, W. Engström, H. List, *In vivo* **2002**, *16*, 229.
[96] a) R. T. Chen, W. Phillips, T. Jannson, D. Pelka, *Opt. Lett.* **1989**, *14*, 892; b) X. Li, J. Zhang, N. Kawazoe, G. Chen, *Polymers* **2017**, *9*, 309; c) K. Yue, G. Trujillo-de Santiago, M. M. Alvarez, A. Tamayol, N. Annabi, A. Khademhosseini, *Biomaterials* **2015**, *73*, 254; d) Z. Wu, X. Su, Y. Xu, B. Kong, W. Sun, S. Mi, *Sci. Rep.* **2016**, *6*, 24474; e) G. Yang, Z. Xiao, X. Ren, H. Long, H. Qian, K. Ma, Y. Guo, *PeerJ* **2016**, *4*, e2497.
[97] M. Märtson, J. Viljanto, T. Hurme, P. Laippala, P. Saukko, *Biomaterials* **1999**, *20*, 1989.
[98] a) K. Lewandowska, A. Sionkowska, B. Kaczmarek, G. Furtos, *Mol. Cryst. Liq. Cryst.* **2014**, *590*, 193; b) A. Sergeev, S. Voznesenskiy, S. Bratskaya, A. Mironenko, R. Lagutkin, *Phys. Proc.* **2012**, *23*, 115; c) E. Szymańska, K. Winnicka, *Marine Drugs* **2015**, *13*, 1819; d) D. Singh, A. Lohade, J. Parmar, D. D. Hegde, P. Soni, A. Samad, M. D. Menon, *Indian J. Pharm. Sci.* **2012**, *74*, 521.
[99] a) J. Kobayashi, T. Asahi, M. Ichiki, A. Oikawa, H. Suzuki, T. Watanabe, E. Fukada, Y. Shikinami, *J. Appl. Phys.* **1995**, *77*, 2957; b) J. S. Bergström, D. Hayman, *Ann. Biomed. Eng.* **2016**, *44*, 330; c) P. Gentile, V. Chiono, I. Carmagnola, P. V. Hatton, *Int. J. Mol. Sci.* **2014**, *15*, 3640; d) S. Lyu, J. Schley, B. Loy, D. Lind, C. Hobot, R. Sparer, D. Untereker, *Biomacromolecules* **2007**, *8*, 2301; e) R. A. Miller, J. M. Brady, D. E. Cutright, *J. Biomed. Mater. Res., Part A* **1977**, *11*, 711.
[100] http://www.kureha.com/pdfs/Kureha-KUREDUX.pdf.
[101] a) J. Buczynska, E. Pamula, S. Blazewicz, *J. Appl. Polym. Sci.* **2011**, *121*, 3702; b) J. Patterson, P. S. Stayton, X. Li, *IEEE Trans. Med. Imaging* **2009**, *28*, 74; c) M. Deng, J. Zhou, G. Chen, D. Burkley, Y. Xu, D. Jamiolkowski, T. Barbolt, *Biomaterials* **2005**, *26*, 4327; d) H. K. Makadia, S. J. Siegel, *Polymers* **2011**, *3*, 1377.
[102] a) Y. Okumura, K. Ito, *Adv. Mater.* **2001**, *13*, 485; b) M. Browning, T. Wilems, M. Hahn, E. Cosgriff-Hernandez, *J. Biomed. Mater. Res., Part A* **2011**, *98*, 268; c) A. K. Gaharwar, C. P. Rivera, C.-J. Wu, G. Schmidt, *Acta Biomater.* **2011**, *7*, 4139.
[103] a) Z. Wang, A. A. Volinsky, N. D. Gallant, *J. Appl. Polym. Sci.* **2014**, 131; b) I. Johnston, D. McCluskey, C. Tan, M. Tracey, *J. Micromech. Microeng.* **2014**, *24*, 035017.